ABSTRACT

Title: ANALYSIS OF HOLD TIMES FOR GASEOUS FIRE SUPPRESSION AGENTS IN TOTAL FLOODING APPLICATIONS

Sean O'Rourke, Master of Science, 2005

Advisor: Frederick W. Mowrer, Associate Professor,

Department of Fire Protection Engineering

Many of the clean agents currently used in total flooding fire suppression applications have vapor densities greater than ambient air. The denser agent-air mixture creates hydrostatic pressure differences causing flow of the mixture out of the enclosure as well as flow of ambient air in through leakage paths inherent in building construction. Hold time refers to the amount of time it takes for the concentration of the agent-air mixture to drop below a specified concentration at a designated height within the protected enclosure. In this study an experimental test enclosure was used to evaluate an analytical model of agent-air mixture leakage and to investigate the effects of different leakage areas on agent hold times. The analytical model, known as the descending interface model, demonstrated favorable agreement with experimental measurements for heights greater than one-half the height of the enclosure for the agent used in this investigation.

ANALYSIS OF HOLD TIMES FOR GASEOUS FIRE SUPPRESSION AGENTS IN TOTAL FLOODING APPLICATIONS

By

Sean Thomas O'Rourke

Thesis submitted to the Faculty of the Graduate School of the
University of Maryland, College Park in partial fulfillment
of the requirements for the degree of
Master of Science
2005

Advisory Committee:

Professor Frederick W. Mowrer, Chair
Professor James Milke
Professor Peter Sunderland

© Copyright by

Sean Thomas O'Rourke

2005

Acknowledgments

This project was supported by 3M's Performance Materials Division. I would like to thank Paul Rivers of 3M for his support and technical guidance while working on this project. Additionally I would like to thank Dr. Frederick Mowrer, my advisor, for his assistance, guidance and time while completing this work.

I would also like to thank the other members of my thesis committee, Dr James Milke, and Dr Peter Sunderland, for their support of this project. Finally, I would like to thank the faculty and staff, as well as my fellow graduate students, in Fire Protection Engineering for their help with this work and my time here at the University of Maryland.

Table of Contents

List of Figures

List of Tables

Chapter 1: Introduction

1.1 Background

The most popular halogenated fire suppression agent, Halon 1301, was developed in the 1960's and quickly saw widespread use in total flooding applications, including the protection of electrical and electronic equipment, process control rooms, and flammable liquid and gas storage and transfer facilities. This widespread application of Halon 1301 quickly came to an end under the Montreal Protocol to protect stratospheric ozone. This agreement among developed countries phased out the production of Halon 1301 as of January 1, 1994 (DiNenno, SFPE Handbook).

As noted by DiNenno (SFPE Handbook p 4-173), the phase out of Halon 1301 led to worldwide research and development efforts in search of suitable replacements and alternatives. Over the past decade many new "halon alternatives" have been developed to fill this gap in technology. These new "clean" agents are similar to Halon 1301 in that they vaporize readily, are electrically nonconductive and leave no residue. These agents fall into two broad categories: halocarbon compounds and inert gases. Some of the commercialized halon alternatives are listed in Table 1.

Table 1 Common Halon Alternatives[a]

Agent Tradename	Chemical Name	ASHRAE designation	Chemical Formula
FE-25	Pentafluroethane	HFC-125	C_2HF_5
FM-200	Heptafluoropropane	HFC-227ea	C_3F_7H
NAF-SII	Dichlorotrifluorethane (4.75%) Chlorodifluoromethane (82%) Chlorotetrafluoroethane (9.5%) Isopropenyl-1-methylcyclohexane (3.75%)	HCFC Blend A	$CHCl_2CF_3$ $CHClF_2$ $CHClFCF_3$
Novec 1230	Dodecafluor-2-methylpentan-3-1	FK-5-1-12	$CF_2CF_2C(O)CF(CF_3)_2$
Argonite	Nitrogen (50%) Argon (50%)	IG-55	N_2 Ar
Inergen	Nitrogen (52%) Argon (40%) Carbon Dioxide (8%)	IG-541	N_2 Ar CO_2

[a]Adapted from SFPE Handbook 3rd Ed p 4-173

Halocarbon clean agents as well as inert gas fire suppression agents extinguish fires by physical and chemical mechanisms that depend on the chemical compound. The dominant suppression mechanism for these agents is the thermal capacity of the gaseous agent that acts as an energy sink to decrease the flame temperature below that needed to sustain combustion. Some of the halogenated compounds extinguish a fire by capturing hydrogen radicals from the fire to interrupt the chemical chain reaction and thus extinguish the fire, but this effect is less pronounced for the halon alternatives than for Halon 1301 (DiNenno, SFPE Handbook).

Since these extinguishing mechanisms occur in the gaseous phase, it is important that the agent concentration necessary to extinguish a fire is maintained for a sufficient period of time to ensure extinguishment. It is assumed that the discharge of the agent initially creates a uniform concentration of agent throughout the enclosure. In real-world enclosures, after the agent is discharged the agent-air mixture will flow through leaks in

enclosure boundaries. Flow through these leaks are mainly attributed to pressure differences due to gas density differences between the inside and outside of the enclosure, as well as to wind or HVAC system effects (Dewsbury and Whiteley p. 249).

One of the many aspects considered when designing clean agent systems is the "hold time" or "retention time" of the enclosure. This time refers to the time it takes for the agent concentration to drop below a specified concentration at a designated height. This height is usually the elevation of the highest potential fire source in the enclosure and the concentration is usually 80% of the minimum design concentration (Dewsbury and Whiteley p. 249). Under current standards the minimum design concentration is typically a factor of 1.2 to 1.3 times the minimum extinguishing concentration (ISO/fDIS 14520.1). A hold time of at least 10 minutes is generally considered desirable to allow items within the enclosure to cool to prevent re-ignition and also to allow manual suppression forces to arrive to take over suppression activities.

There are two generally recognized models of leakage through enclosure boundaries, the descending interface model and the continuous mixing model. Experiments conducted by Dewsbury and Whiteley in 2000 captured the flow behavior of Halon 1301. Dewsbury and Whiteley conclude with the statement, "Further research is required to determine what interface concentration profiles are found in practice, with a wide variety of enclosures and agents" (Dewsbury and Whiteley p. 275).

1.2 Description of Total Flooding Application

A representative total flooding fire suppression system is shown in Figure 1. An enclosure is equipped with an automatic fire detection system that triggers the activation of the fire suppression system. The fire suppression system consists of pressurized

cylinders containing the fire suppression agent, piping, and sufficient nozzles to ensure prompt and uniform agent delivery throughout the enclosure. Upon system activation, the agent flows from the storage cylinders, through the system piping and is discharged from the nozzles, typically 10 seconds. The objective of the system is to quickly achieve concentration of agent throughout the enclosure volume that is sufficient to extinguish flaming fires within the enclosure.

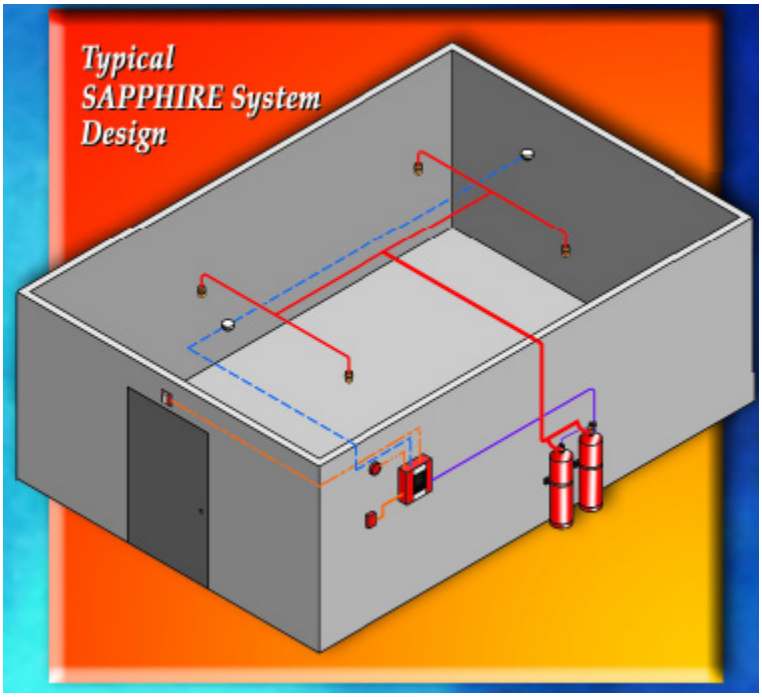

Figure 1 Schematic of Total Flooding Clean Agent Application
(3M Novec 1230 Product Brochure)

Once the agent is uniformly dispersed within the enclosure, the agent concentration will start to decrease due to flow through leakage paths in the enclosure boundaries. The rate of leakage depends on the areas and locations of the leakage paths as well as the density of the agent-air mixture. Two models have been previously developed to evaluate this leakage: the descending interface model and the continuous mixing model.

1.3 Project Objectives

The primary goal of this project is to compare experimentally measured agent concentrations at different elevations with those predicted by the theoretical models. This study evaluates the existing leakage theories as they apply to the leakage behavior of Novec 1230, one of the Halon 1301 replacements currently being used. To achieve this goal an experimental enclosure has been constructed to measure the agent concentrations at three elevations and thus calculate leakage flows into and out of the enclosure. These measurements and calculations are compared with those predicted by the theoretical models. The effect of different upper and lower leakage areas on the flow characteristics is investigated by varying the leakage areas. All of the experimental data as well as the theoretical predictions are expressed in dimensionless form to allow comparisons among different enclosure and agent characteristics.

Chapter 2: Theoretical Considerations

2.1 Literature Review

Some of the first work on the issue of hold or retention time of enclosures was done by DiNenno and Forssell (1989). Although their work was done prior to the Montreal Protocol, they recognized that restrictions on Halon 1301 usage were imminent and therefore wanted to develop an alternative to the total flooding discharge tests that were being conducted.

DiNenno and Forssell developed the door fan pressurization test method currently used to estimate the leakage rate from an enclosure. Because the details of leaks and cracks around doors, windows, vents, pipes and electrical conduit are rarely known this method found an equivalent leakage area over the compartment boundary. During a room integrity test, a calibrated fan injects (or removes) air at a known flowrate into (or from) a room and the consequent increase (or decrease) in pressure is then measured. These flowrate and pressure measurements are repeated at a number of flowrates and from these data the leakage characteristics of the enclosure are determined based on orifice flow theory.

In order to predict the leakage rate following agent discharge, a distribution of the leakage area over the compartment boundaries must be assumed. This leakage area is expressed as the equivalent area of flow through a sharp-edged orifice. The effective leakage area is found by dividing the actual leak area equally between the ceiling and floor of the enclosure. This assumption is made because it maximizes the leakage rate and consequently minimizes the hold time (Dewsbury and Whiteley, p. 267).

The ratio of the leakage assigned to the floor to the total leakage area is known as the lower leakage fraction, F_a. When F_a is approximately 0.5, the fastest descent of the interface will occur. This is therefore the most conservative distribution of the actual leaks if an assumption is needed (Dewsbury and Whiteley, p. 267).

The equations that DiNenno and Forssell developed for the descending interface are based on the pressure and density differences that develop within the enclosure after agent discharge. These pressure differences are raised to a power N which is determined experimentally through the fan pressurization test. They state that the simplest relation is if the pressure differences are raised to the one-half power from argument of the derivation of Bernoulli's equation. They mention that the actual value of the power can vary from 0.5, depending on the actual flow characteristics of the enclosure (DiNenno and Forssell 1989).

DiNenno and Forssell conducted sixteen fan pressurization experiments with different known leakages and fan flowrates in an experimental enclosure. The results from these experiments showed that the fan pressurization test is an effective way to find an equivalent leakage area of an enclosure. These experiments also yielded values of the exponent N of approximately 0.5 as expected from orifice flow theory.

The current NFPA standard on clean agent suppression systems is NFPA 2001, 2004 edition (NFPA, 2004). In this standard the design criteria for clean agent fire suppression systems are outlined. Annex C of NFPA 2001 outlines the procedure to test the integrity of an enclosure. The room integrity test is similar to that described by DiNenno and Forssell where an equivalent leakage area is a theoretical sharp-edge orifice of all leaks within the enclosure. For the flow equations used in this standard an orifice

coefficient (C_d) of 0.61 is used. The value of the leakage exponent, N, is assumed to be 0.5. This orifice coefficient is that of turbulent flow through a sharp-edged orifice.

Similar to NFPA 2001, ISO/fDIS 14520.1 is the international standard governing clean agent systems (ISO/fDIS 14520.1, 2003). The section of the standard applicable to hold time calculations is Annex E. A door fan test is also used to determine the minimum hold time of an enclosure. In the equations for hold time, ISO/fDIS 14520.1 also assumes an orifice coefficient of 0.61. Unlike NFPA 2001, ISO/fDIS 14520.1 requires the value of the leakage exponent to be determined experimentally through the fan pressurization test. Equations for both the uniformly mixed and sharp descending interface models for leakage are provided.

2.2 Hydrostatic Pressure Profile within an Enclosure

The discharge of a clean agent into an enclosure is highly turbulent and develops a relatively uniform agent-air mixture throughout the enclosure. Because most agents have vapor densities greater than that of air, the mixture density is greater than that of the air surrounding the enclosure. This heavier-than-air mixture exerts a positive hydrostatic pressure on the lower part of the enclosure boundaries. This pressure causes the mixture to flow out of leakage paths located in the lower part of the enclosure.

Since the enclosure is of fixed volume the leakage of agent-air mixture from the enclosure creates a reduced hydrostatic pressure near the top of the enclosure. This causes ambient air to flow into the enclosure via leakage paths in the top of the enclosure. The fixed enclosure volume results in a quasi-steady state condition where the volumetric flowrates into and out of the enclosure are equal. The pressure differences at the top and

bottom of the enclosure are used to calculate volumetric flowrates as discussed in Section 2.3.

A schematic of the hydrostatic pressure profile in an enclosure is presented in Figure 2. The gray area designates the homogeneous agent-air mixture with density ρ_m. The height of this mixture, h(t), descends as the mixture flows out of the enclosure and ambient air flows in to replace the outflowing mixture. Figure 2 also schematically shows the inside and outside pressure profiles. A neutral plane at height n(t) exists at the elevation where inside and outside pressures are the same.

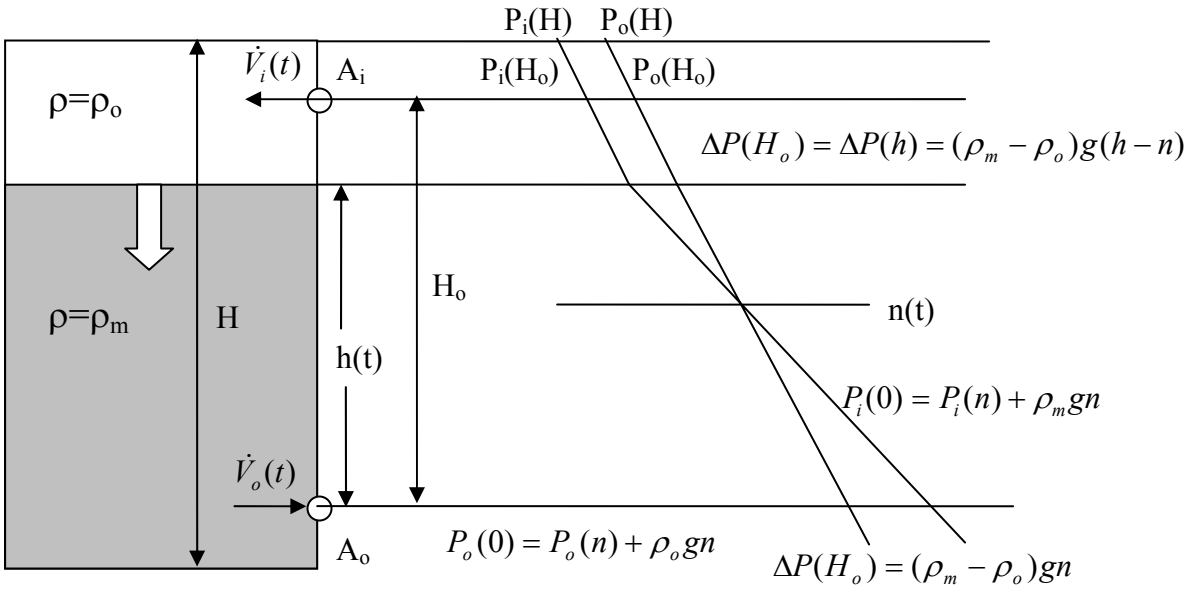

Figure 2 Hydrostatic Pressure Profile Schematic

2.3 Leakage Area and Flowrate

The volumetric flowrates into and out of the enclosure are governed by the hydrostatic pressure differences at the upper and lower leakage paths. These pressure differences are due to density differences between the agent-air mixture and the air

surrounding the enclosure. An equation for the volumetric flowrate into or out of an enclosure is expressed as

$$\dot{V} = C\left(\frac{2\Delta P}{\rho_{air}}\right)^{N} \qquad \text{Equation 1} \qquad \text{(DiNenno and Forssell p 131)}$$

Where $C = K_d A_T K_U$

This equation assumes that there are no obstructions near the inlet or outlet, the plate thickness is small compared to the orifice diameter, changes in temperature and absolute pressure are small, and flow through the orifice is turbulent. The constant, C is based on the orifice coefficient, K_d the discharge coefficient, , A_T the leakage area, and a constant Ku which is based on the value of N and the units being used.

The orifice coefficient is the ratio of the actual flow to the theoretical maximum flow. This value is 0.61 for sharp-edge circular orifices, the value used in NFPA 2001. The value of N will vary for actual leaks in enclosure boundaries. In general, the value of N can be taken as 0.5 based on Bernoulli's equation, and is applicable for laminar flow through small orifices (DiNenno and Forssell p 133). This value of N is used in the current NFPA 2001 standard and will therefore be used in the theoretical analysis for this project.

2.4 Flow Models

Halon alternatives are generally denser than air and consequently will flow out of leaks inherent in building construction. There are three accepted models for this leakage: the sharp descending interface model, the continuous mixing model, and the wide interface model. The sharp interface and continuous mixing models are described in the literature by DiNenno and Forssell (1989) as well as used in the NFPA 2001 and

ISO/fDIS 14520.1 standards. The wide interface model was developed more recently by Dewsbury and Whiteley (Dewsbury and Whiteley, 2000). In subsequent sections these models will be manipulated and rendered dimensionless to permit comparisons over a range of conditions.

2.4.1 Descending Interface Model

The first model to be described for the leakage behavior is the descending interface model (DiNenno and Forssell 1989). This model is usually applied to halon alternatives because of their high vapor densities. In this model it is assumed that a constant and uniform concentration of agent-air mixture exists after discharge. This mixture is denser than the air outside the enclosure and therefore flows out of the lower leakage paths. As the mixture flows out of lower leaks due to hydrostatic pressure created by the mixture, air from outside the enclosure flows in from leaks in the top of the enclosure. This pressure difference at the top of the enclosure draws air in to replace the agent-air mixture leaving from the bottom of the enclosure. The volumetric flowrates into and out of the enclosure are equal because the volume of the enclosure is fixed. The agent-air mixture stays at constant concentration, but the height of this layer descends over time.

The volumetric flow rate into or out of the enclosure is a function of the orifice area, height of the enclosure, as well as pressure and density differences between the agent-air mixture within the enclosure and the ambient air surrounding the enclosure. The height of the layer is a major factor governing the flow. A tall layer will create more hydrostatic pressure and as the layer descends, the hydrostatic pressure differences at the lower leakage paths will decrease, reducing the volumetric flowrates over time. An

equation relating these volumetric flowrates to the hydrostatic pressure differences within the enclosure are expressed as Equation 2 and Equation 3 respectively.

$$\dot{V}_i = C_i A_i \sqrt{\frac{2\Delta P(h)}{\rho_o}} = C_i A_i \sqrt{\frac{2g(h-n)\Delta\rho}{\rho_o}} \qquad \text{Equation 2}$$

$$\dot{V}_o = C_o A_o \sqrt{\frac{2\Delta P(0)}{\rho_m}} = C_o A_o \sqrt{\frac{2gn\Delta\rho}{\rho_m}} \qquad \text{Equation 3}$$

A dimensionless expression relating the neutral plane, the height at which there is no hydrostatic pressure difference, to the overall enclosure height can be found by equating the inlet and outlet flowrates and then rearranging.

$$\frac{N}{H} = \frac{1}{1+\left(\frac{\rho_o}{\rho_m}\right)\left(\frac{C_o A_o}{C_i A_i}\right)^2} \qquad \text{Equation 4}$$

This expression can then be substituted into the volumetric outlet flowrate equation (Equation 5) for a new expression of the volumetric outflow rate.

$$\dot{V}_o = C_o A_o \sqrt{\frac{2\Delta\rho g h(t)}{\rho_m\left[1+\left(\frac{\rho_o}{\rho_m}\right)\left(\frac{C_o A_o}{C_i A_i}\right)^2\right]}} = k_1\sqrt{h(t)} \qquad \text{Equation 5}$$

where $k_1 = C_o A_o \sqrt{\frac{2\Delta\rho g}{\rho_m\left[1+\left(\frac{\rho_o}{\rho_m}\right)\left(\frac{C_o A_o}{C_i A_i}\right)^2\right]}} = C_o A_o \sqrt{\frac{2\left(1-\frac{\rho_o}{\rho_m}\right)g}{\left[1+\left(\frac{\rho_o}{\rho_m}\right)\left(\frac{C_o A_o}{C_i A_i}\right)^2\right]}}$

The rate of descent of the interface layer can be represented by the following differential equation, where A_c is the cross-sectional area of the enclosure, assumed to be constant.

$$\frac{dh(t)}{dt} = \frac{-\dot{V}_o(t)}{A_c} = \frac{-k_1}{A_c}\sqrt{h(t)} \qquad \text{Equation 6}$$

Equation 6 is integrated from H_o to h(t) and from t_o to t, the height of the interface at a given time can be found, where t_o is the time when the interface reaches H_o.

$$\int_{H_o}^{h(t)} (h)^{-1/2}\, dh = \frac{-k_1}{A_c}\int_{t_o}^{t} dt \Rightarrow \left(\frac{h(t)}{H_o}\right)^{1/2} = 1 - \frac{k_1(t-t_o)}{2A_c\sqrt{H_o}} \qquad \text{Equation 7}$$

To make Equation 7 nondimensional, a characteristic volumetric flowrate ($\dot{V}_C$) and a characteristic drain time τ are defined.

$$\dot{V}_C \equiv C_o A_o \sqrt{gH_o} \qquad \text{and} \qquad \tau \equiv \frac{V_o}{\dot{V}_C} = \frac{A_c H_o}{C_o A_o \sqrt{gH_o}} = \left(\frac{A_c}{C_o A_o}\right)\left(\sqrt{\frac{H_o}{g}}\right)$$

When these terms are substituted into Equation 7 the nondimensional form of the interface height is given by Equation 8.

$$\frac{h(t)}{H_o} = \left[1 - \frac{k_2(t-t_o)}{\tau}\right]^2 \qquad \text{Equation 8}$$

where $$k_2 = \left[\frac{\left(1-\frac{1}{\tilde{\rho}}\right)}{2(1+\frac{1}{\tilde{\rho}}\tilde{A}^2)}\right]^{1/2} \qquad \tilde{\rho} = \frac{\rho_m}{\rho_o} \qquad \tilde{A} = \left(\frac{C_o A_o}{C_i A_i}\right)$$

Thus, the parameters governing the rate of descent of the descending interface includes the mixture density relative to the ambient density, the ratio between the outlet and inlet leakage path areas, the ratio between the enclosure floor area and the outlet leakage path area, and the height between the inlet and outlet leakage paths.

2.4.2 Continuous Mixing Model

The second widely recognized model is the continuous mixing model (DiNenno and Forssell 1989). In this model, the air that enters the enclosure mixes with the agent-air mixture, decreasing its concentration over time. Because of this constant mixing a well-

defined interface is not formed. This flow behavior is dominant for the lighter halon alternatives, mainly the inert gas agents, that have molecular weights comparable to air. These lighter agents do not form the dense homogeneous mixture and therefore mix easier.

In this model, instead of a descending interface, the concentration decreases uniformly throughout the enclosure over time. For the calculation of hold times using the continuous mixing model, the same equations are used to find the volumetric flowrates using an equivalent height of mixture to represent the reduced agent-air concentration.

$$t = \frac{A_s H}{F_a C_d} \int_{\rho_{mi}}^{\rho_m(t)} \left[\frac{2gH(\rho_m - \rho_a)}{\rho_m + \left[\frac{F_a}{1 - F_a} \right]^2 \rho_a} \right]^{-1/2} d\rho_m \qquad \text{Equation 9}$$

Equation 9 is integrated from the initial agent-air mixture density ρ_{mi} to a given mixture density $\rho_m(t)$.

2.4.3 Wide Interface

Another model of flow behavior is a combination of the descending interface and the continuous mixing model (Dewsbury and Whiteley 2000). The previous descending interface model assumed a sharp interface between the air-agent mixture and pure air. Dewsbury and Whiteley hypothesizes that even in the absence of good mixing within the enclosure, an interface gradient exists rather than the sharp interface assumed by DiNenno and Forssell (Dewsbury and Whiteley p 271). The interface between the air and homogeneous mixture goes from initial concentration to ambient air as one moves up along the interface. Therefore the bottom of the interface is where the agent-air

concentration is equal to the initial value and the top of the interface is the location of ambient air. If the interface is narrow compared to the height of the enclosure, the error introduced by ignoring this gradient is small. Conversely, if it is large compared to the height of the enclosure then its effect on hold time should be considered.

The bottom of a wide interface descends faster than that of a sharp interface at a given height due to the additional column pressure of the agent in the wide interface. Additionally, agent is now removed from the mixture by adding to the wide interface as well as flowing out of the enclosure via lower leakage paths, decreasing the hold time and increasing the rate at which the layer descends.

This behavior of a wide interface was shown by tests conducted by Klocke (1998). A conclusion drawn in his paper is that a clear borderline does not exist under real conditions. The measured hold times were generally much shorter than those predicted by the sharp descending interface or continuous mixing models.

Myint (1991) proposed a stepwise approximation of an interface with a linear concentration profile. If H_i denotes the height of the top of the agent-air mixture at the initial discharge concentration, r_c is the ratio of the mean agent concentration from H_i to H_o to the concentration of the homogeneous agent-air mixture, the new representative height of the wide interface is:

$$H = H_i + r_c(H_o - H_i) \qquad \text{Equation 10}$$

This new height can be then used in the previously presented equations for the sharp descending interface.

2.5 Other Considerations

In some instances, differences between the inside and outside temperature exist. Correction factors can be added to the volumetric flowrate calculated via Equation 11 to correct for these differences.

$$\dot{V}_{Cor} = \dot{V}\left(\frac{P_{calc}}{P_{ref}}\right)^{0.5}\left(\frac{T_{ref}}{T_{calc}}\right)^{0.5}\left(\frac{T_{leak}}{T_{fan}}\right)^{0.5} \qquad \text{Equation 11}$$

The final correction made to the volumetric flowrate equation is for bias pressure. A bias pressure is positive or negative pressure gradient between the enclosure and the surroundings created by HVAC systems, wind, or temperature differences. The bias pressure is usually small (Dewsbury and Whiteley p254) and will therefore not be considered in detail.

2.6 Agent-Air Density

When the agent is discharged into the enclosure, it is assumed that the agent and air are initially well mixed. The density of this mixture, ρ_m, is usually larger that that of ambient air and thus plays a large role in the flow of the mixture out of the enclosure through leak. This density can be found via Equation 12 where V_d is the agent vapor density, C is the molar percent concentration of the agent, and ρ_a is the air density. The ratio between the agent-air density and that of the air surrounding the enclosure will govern the flow behavior of the mixture.

$$\rho_m = V_d \frac{C}{100} + \left[\rho_o \frac{(100 - C)}{100} \right] \qquad \text{Equation 12}$$

Equation 12 can be nondimensionalized by dividing both sides by the ambient air density, ρ_o.

$$\tilde{\rho} = \frac{\rho_m}{\rho_o} = \frac{V_d}{\rho_o} \frac{C}{100} + \left[\frac{100 - C}{100} \right] \qquad \text{Equation 13}$$

The vapor density of most halon alternatives is greater than that of air. The density ratio, which is the ratio of the agent-air mixture density to that of ambient air, will affect the hold time of the agent-air mixture within the enclosure. Table 2 lists the mixture densities, density ratios and the velocity ratios for the clean agents listed in Table 1. It shows that the inert gases, IG-541 and IG-55, have density ratios between 1.07 and 1.08, while the halocarbon agents have density ratios between 1.28 and 1.43.

Table 2 Clean agent density and velocity ratios[a]

Agent	Vapor density	Cup burner concentration	Design concentration	Mixture density	Density ratio	Velocity ratio
	(kg/m^3)	(Vol. %)	(1.3 * CB conc)	(kg/m^3)	(ρ_m / ρ_a)	V_o/V_c
FK-5-1-12	13.66	4.5	5.85	1.934	1.605	0.48
HCFC blend A	3.84	9.9	12.87	1.544	1.281	0.35
HFC-125	5.06	8.7	11.31	1.641	1.362	0.39
HFC-227ea	7.26	6.6	8.58	1.725	1.431	0.42
IG-541	1.41	31	40.3	1.288	1.069	0.18
IG-55	1.41	35	45.5	1.298	1.077	0.19

[a]Adapted from SFPE Handbook 3rd Ed p 4-173

If the upper and lower leakage areas are equal the velocity ratio for agent-air mixture with different density ratios out of the enclosure can be represented as Equation 14.

$$\frac{v_o}{v_c} = \left[\frac{1-\tilde{\rho}^{-1}}{1+\tilde{\rho}^{-1}}\right]^{1/2} \qquad \text{Equation 14}$$

where this characteristic velocity is equal to $v_c = (2gh)^{0.5}$

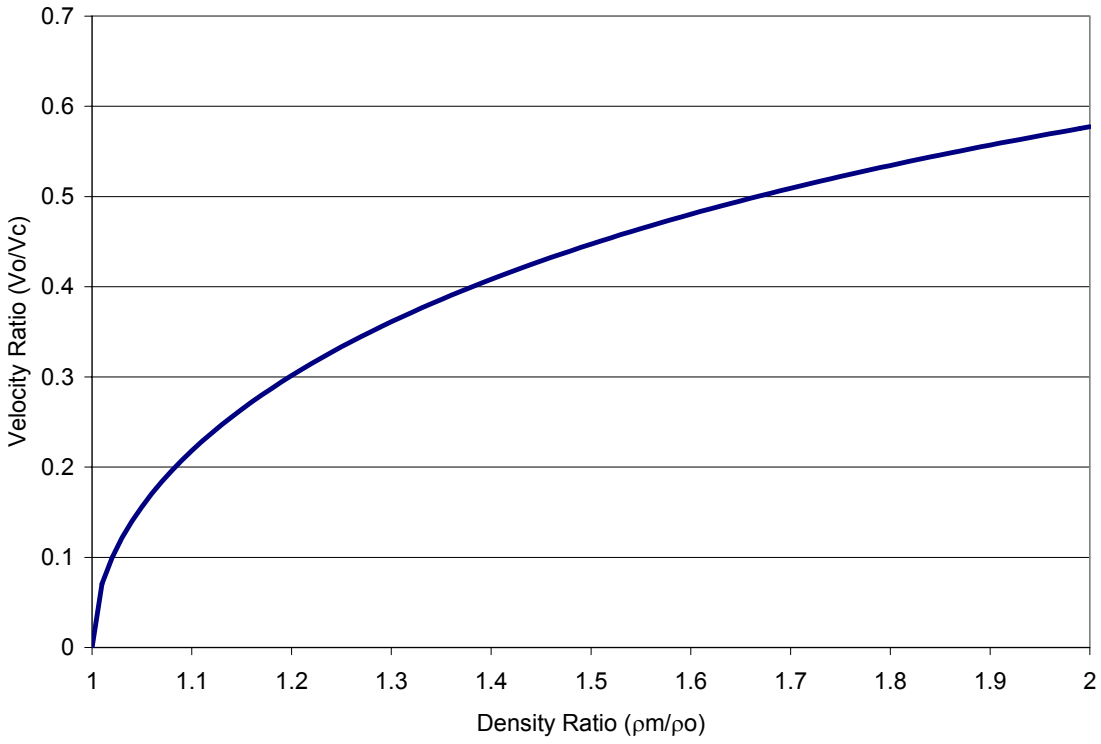

Figure 3 Effect of density ratio on velocity ratio

As shown in Figure 3 the density ratio, $\tilde{\rho}$, has an effect on the flow of the agent-air mixture out of the enclosure. An increase in agent vapor density increases the expected flowrate of mixture out of the enclosure, thus decreasing the hold time of the agent-air mixture within the enclosure. The clean agents with higher agent-air mixture densities at the design concentration will yield smaller hold times.

2.7 Leakage Area

Another parameter that has an effect of the hold time on an enclosure is the leakage ratio. In addition to the total area available for agent to leak out of the enclosure and ambient air to flow into the enclosure, the ratio of the upper and lower leakage areas will also play a role in the leakage flow behavior. DiNenno and Forssell (1989) define the leakage ratio as F_a, the ratio of the lower leakage area (A_o) to the total effective leakage area (A_o+A_i). They report that the minimum hold time should occur when F_a is approximately equal to 0.5.

The effect of the quantity F_a on the hold time is graphically shown in Figure 4, where the hold time at a height of half the original height is plotted as a function of F_a. Based on this graphical representation, the minimum hold time occurs at values of F_a just above 0.5.

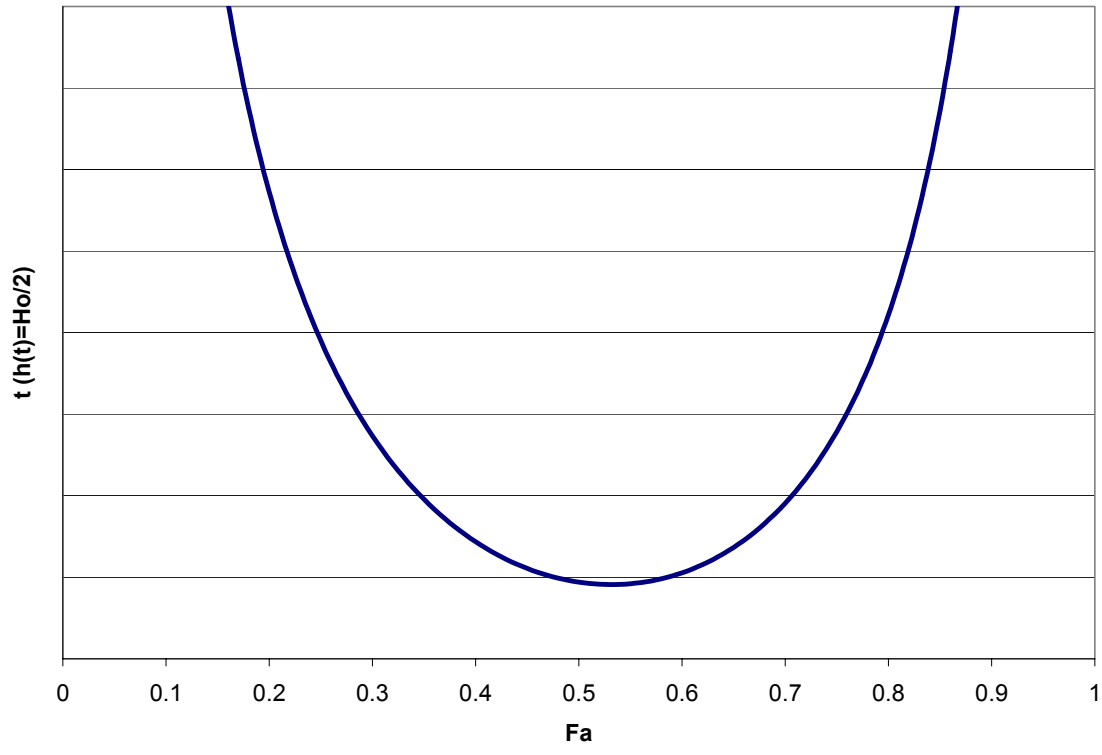

Figure 4 Effect of Area Ratio DiNenno and Forssell Analysis

The area ratio used in the dimensionless analysis is A_o/A_i. The effect of this area ratio on the hold time is shown in Figure 5. Although this ratio does not take total leakage area into account, it is assumed that the total leakage area stays equal for all cases. The area ratio is plotted on a logarithmic scale. Similar to the DiNenno and Forssell analysis, the minimum hold time occurs when the outlet area is slightly larger than the inlet area.

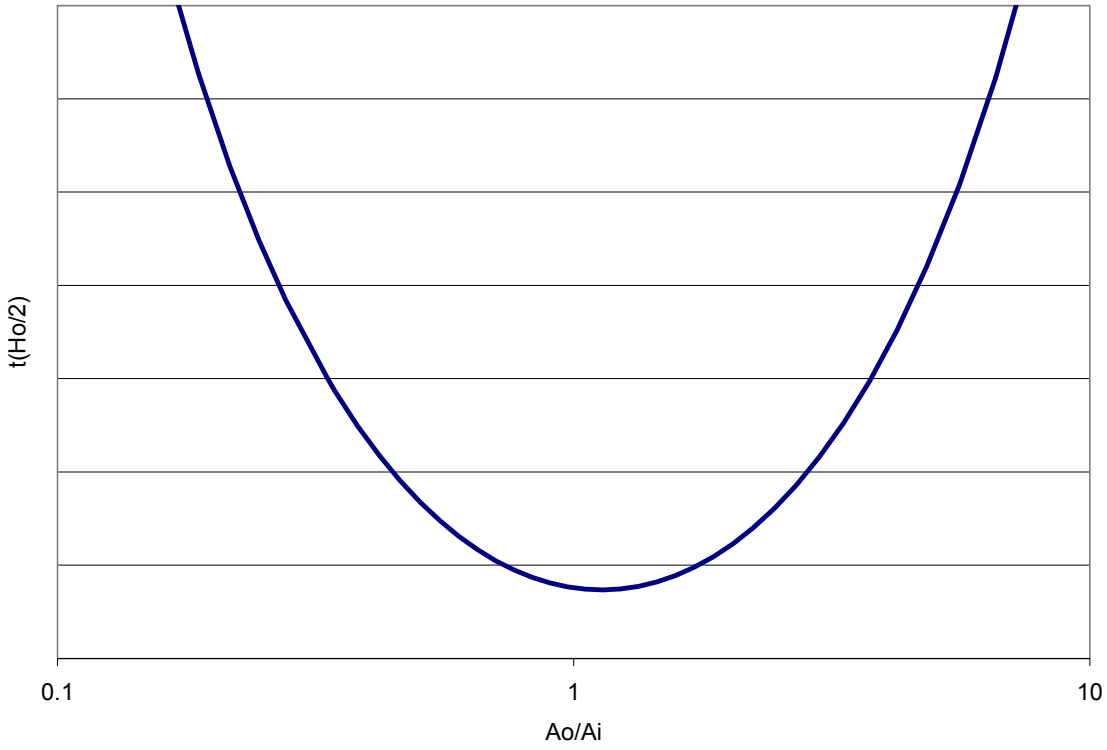

Figure 5 Effect of Area Ratio Dimensionless Analysis

Chapter 3: Experimental

3.1 Test Apparatus Description

The purpose of these experiments was to investigate the flow behavior of clean agents from an enclosure. To do this a test enclosure was made out of acrylic plastic. The enclosure was a vertical cylinder with a height of 1.83 m, a diameter of 0.61 m and an internal volume of 0.534 m^3. A number of 12.7 mm diameter holes were drilled into the side of the enclosure for instrumentation and leakage purposes. Three equally-spaced holes were located at a height of 1.68 m to serve as the upper leakage paths. Three holes at a height of 0.077 m served as the lower leakage paths. The lower and upper leakage areas could be increased or decreased by plugging one or more of the holes. A schematic of the test apparatus is shown in Figure 6.

Agent was discharged into the enclosure through a 500 cm^3 sample cylinder and ¼ in NPT pipe (ID=9.2 mm). Liquid agent was added to the cylinder and then pressurized to approximately 2.48 MPa (360 psig) with nitrogen to closely mimic field conditions. A ball valve isolated the pressurized cylinder from the discharge piping and, when opened, would quickly discharge the agent into the enclosure. Two inline pressure transducers were placed within the piping to measure the pressure. The first was connected to the sample cylinder to measure its pressure. The second was placed at the connection right before the pipe entered the test enclosure to measure the pressure at discharge and to signal the beginning of a test. A Bete NF1000 discharge nozzle was selected through trial and error so that the discharge time would be approximately 10 seconds per the NFPA 2001 standard. A schematic of the agent delivery system is shown

in Figure 7. Figure 8 shows a picture of the actual experimental apparatus and the agent delivery system.

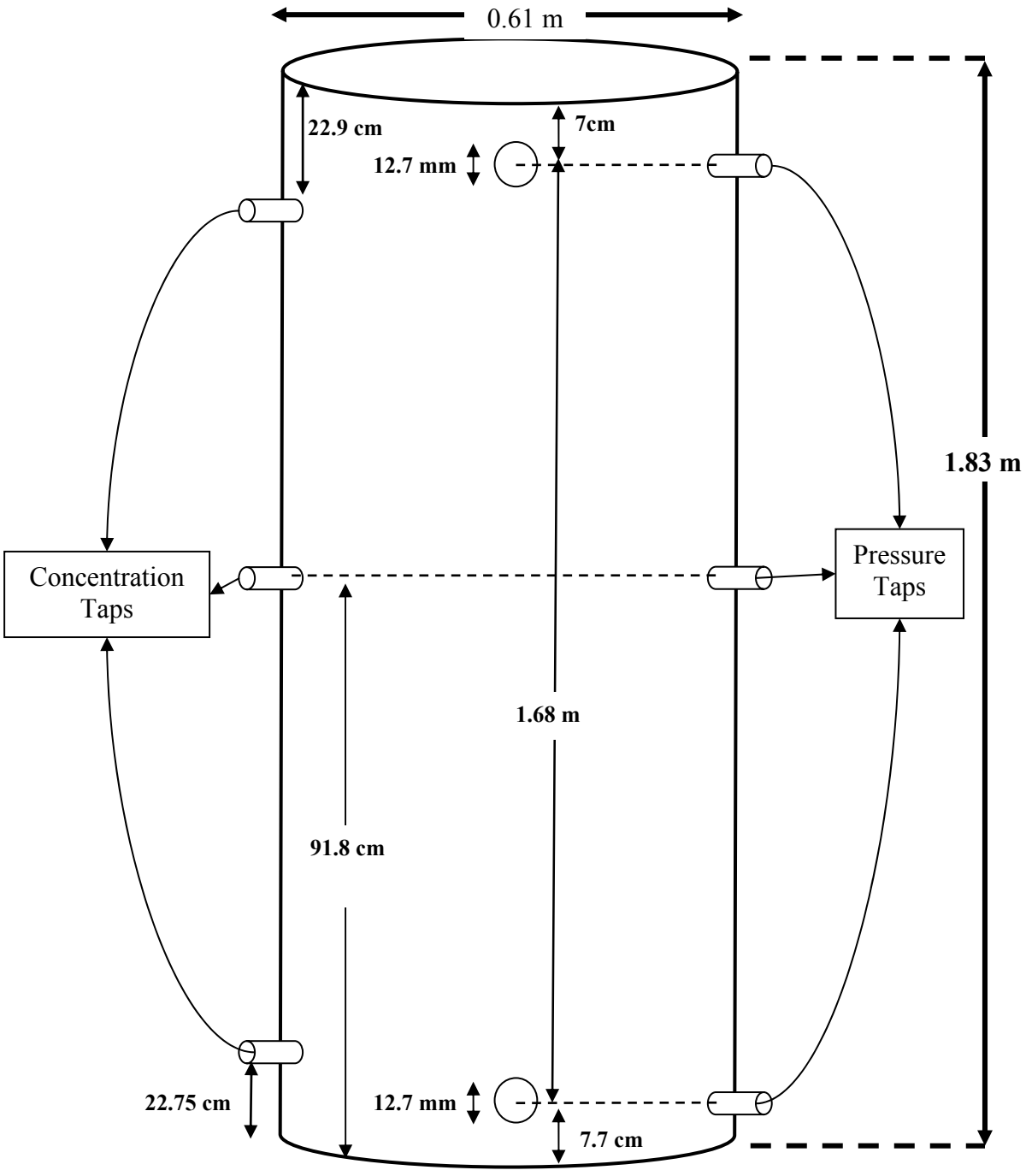

Figure 6 Schematic of Test Apparatus, elevation view

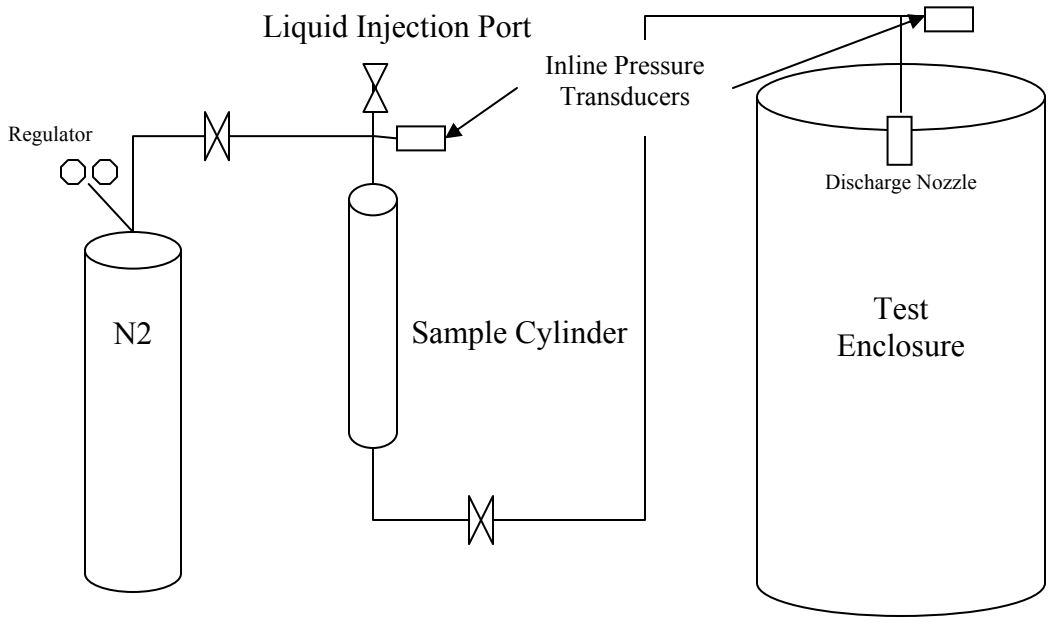

Figure 7 Schematic of Agent delivery system

a **b**

Figure 8 Photograph of (a) Test Apparatus and (b) Agent Delivery System

Three concentration sampling ports were located at 168 cm, 91.8 cm, 23 cm from the bottom of the enclosure. These ports were connected via plastic tubing to a Tripoint Analyzer which measured the agent concentration at the specified heights during a test. Other instrumentation included three pressure transducers located at 1.68 m, 0.92 m, and 0.15 m which measured the pressure differential between the inside and outside of the enclosure. The upper and lower pressure transducers are located at the same elevations as the upper and lower leakage paths. A Type K Thermocouple was also placed in the agent discharge stream to measure the changes in temperature within the enclosure. A data acquisition unit was used to record all instrumentation measurements during the test at a sampling rate of 1 Hz.

Figure 9 Agent Discharge Nozzle

3.2 Experimental Methodology

The design concentration for Novec 1230 is 4-6% by volume (3M Performance Materials Division p. 3). The experiments were conducted with the high-end design concentration of 6% for maximum flow and therefore minimum hold time. To determine the amount of liquid agent that was needed to achieve the design concentration within the test enclosure, Equation 15 was used, where V is the volume of the enclosure, s is the specific volume of the superheated agent vapor, and C is the design concentration.

$$W = \frac{V}{s}\left(\frac{C}{100 - C}\right) \qquad \text{Equation 15} \qquad \text{(NFPA 20001, p 2001-15)}$$

As given in NFPA 2001 (p 2001-51), the specific volume of the Novec 1230 vapor at room temperature (25 ºC) is 0.0732575 m^3/kg. Substituting these quantities into Equation 15, it is found that 0.465 kg of Novec 1230 is required to achieve an agent molar concentration of 6% in the test enclosure. With a liquid density of 1.6 g/m, for Novec 1230, the volume of liquid agent needed for each experiment is 285 mL to achieve a design concentration of 6.0%.

The required amount of liquid agent was added to the sample cylinder and all valves were closed. The cylinder was than charged to approximately 4.8 MPa with compressed nitrogen. The sample cylinder was shaken a number of times to allow some nitrogen to go into solution with the liquid Novec 1230. After each shake the cylinder was re-pressurized to 4.8 MPa. The cylinder was then reconnected to the agent delivery system. This process was repeated approximately five times. The Tripoint analyzer and data acquisition system were started to begin data collection. When sufficient time had elapsed for the Tripoint Analyzer to warm-up and for baseline data to be collected, the

ball valve isolating the sample cylinder from the discharge piping to the enclosure was opened and discharge occurred for approximately 10 seconds. The concentration at all three sample ports as well as temperature and pressure differences were measured every second for the duration of the test.

Experiments with five different area leakage scenarios were conducted to investigate the effect of the leakage area and the leakage area ratio on the flow of the agent-air mixture out of the enclosure. The first three sets of experiments had equal upper and lower leakage areas of 0.00038 m^2, 0.000253 m^2, and 0.000127 m^2 respectively. The next set of experiments had an upper leakage area of 0.00038 m^2 and lower leakage area 0.000127 m^2. The final set of experiments had an upper leakage area of 0.000127 m^2 and a lower leakage area of 0.00038 m^2. Table 3 summarizes the experiments conducted.

In order to validate the leakage area scenarios presented in Table 3, the ratio of the total leakage area to the surface area of the enclosure can be compared to that found in actual buildings. Klote and Milke report the tightness of actual comerical buildings: an area ratio of 0.50E10-4 as a tight bulding, 0.17E-3 as an average building, and 0.35E-3 as a loose building. All of the experiments conducted in this project fall within the criteria of tight or average tightness.

Table 3 Comparison of Leakage Area Scenarios

Area Leakage Scenario	# of Experiments Conducted	A_o (m^2)	A_i (m^2)	A_T (m^2)	Area Ratio	Tightness
1	3	0.00038	0.00038	0.00076	2.00E-04	Average
2	2	0.000253	0.000253	0.000506	1.33E-04	Average
3	4	0.000127	0.000127	0.000254	6.69E-05	Tight
4	2	0.000127	0.00038	0.000507	1.34E-04	Average
5	2	0.00038	0.000127	0.000507	1.34E-04	Average

Chapter 4 Results and Discussion

4.1 Agent Discharge

In order to closely represent an actual discharge that would occur in the field, a discharge time of approximately 10 seconds was desired. A BETE NF1000 nozzle was selected to meet this discharge time criteria. Evidence of the 10 second discharge time is shown in Figure 10 with a sharp increase in pressure at the nozzle and a sharp decrease in pressure within the agent discharge cylinder for approximately 10 seconds.

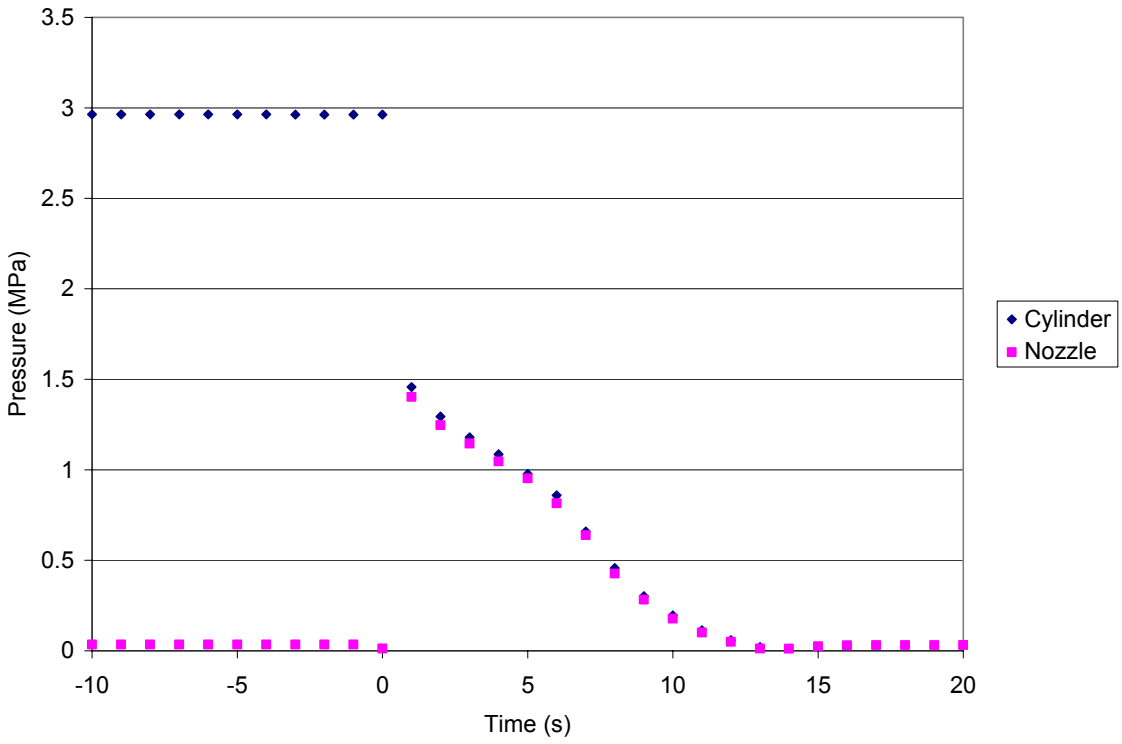

Figure 10 Inline Pressure Profiles

The discharge of agent into the enclosure causes a decrease in temperature throughout the enclosure as the agent is vaporizing. After the initial drop in temperature the agent-air mixture increases in temperature to that of the surroundings, approximately 26ºC. To measure this temperature profile, two thermocouples were placed in the

enclosure, one in the agent discharge stream and the other near the center of the enclosure. Time-temperature histories generated by the thermocouples are shown in Figure 11 for one of the experiments.

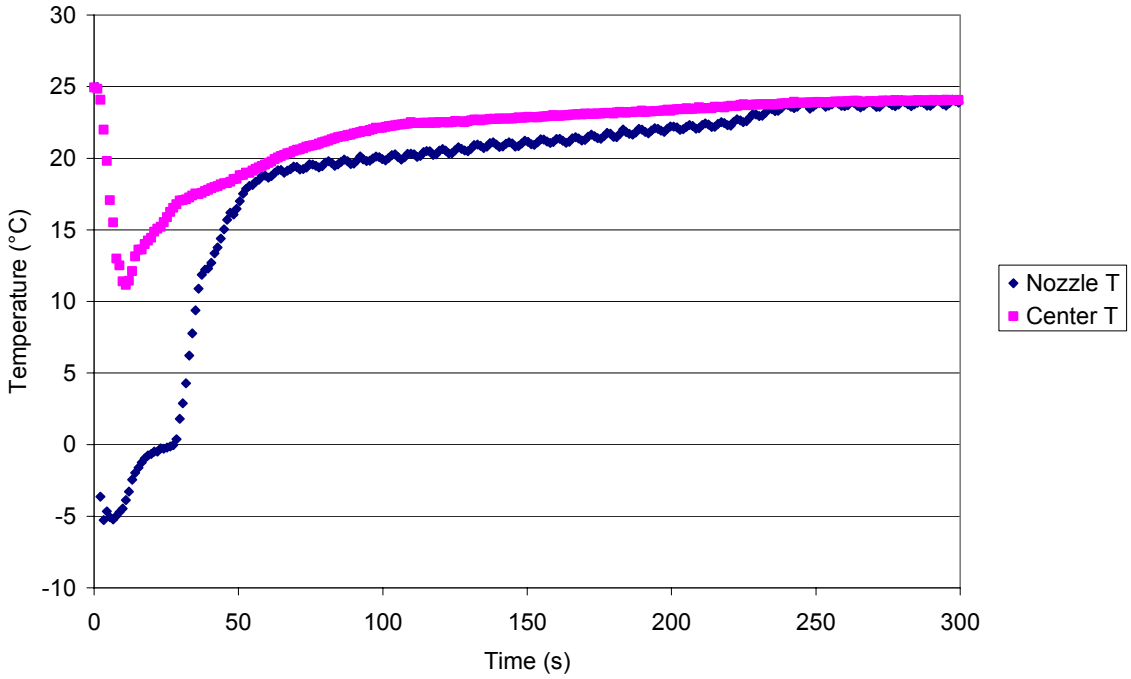

Figure 11 Temperatures within the enclosure

4.2 Concentration Profiles

The primary purpose of these experiments was to evaluate how well the theoretical model predicts the flow characteristics of the Novec 1230-air mixture out of an enclosure. Although an agent mole fraction of approximately 6% was desired, the measured agent mole fraction after discharge throughout the enclosure was consistently at approximately 4.7%. This reduced mole fraction could be a result of the entire amount of liquid agent not discharging from the sample cylinder. The Tripoint analyzer measured the concentration at three elevations approximately every four seconds. These

readings provided a time-concentration profile at 1.6, 0.92, and 0.23 m within the chamber. A set of characteristic time-concentration profiles for each set of experiments is shown in this section. Profiles from experiments with the same leakage area conditions as well as raw data are provided in Appendix A for all experiments.

Figure 12 shows the time-concentration profile for a discharge test with 0.00038 m^2 leakage areas in both the upper and lower leakage paths. The concentration profiles support the assumption of uniform agent-air concentration throughout the enclosure after discharge. For these experiments the initial concentration throughout the enclosure was 4.7%. After the enclosure reaches uniform concentration an interface layer forms and begins to descend within the enclosure. The leading edge of the interface reaches the first concentration port at a height of 1.6 m 116 seconds after the end of discharge. For these experiments, the leading edge of the interface is defined as 80% of the initial concentration. It takes 29 seconds for the trailing edge of the interface to reach the sample port. The trailing edge is defined as 20% of the initial concentration.

The driving force of the descending interface is the hydrostatic pressure profile. As the interface descends, this driving force decreases as shown in the hydrostatic pressure profiles presented in the next section. This trend is shown as the descending interface takes more time to pass through the lower concentration sample ports. This wider shape of the descending interface is greatest at the lowest port where it takes 1099 seconds for the trailing edge of the interface to drop below sampling height of .223 m.

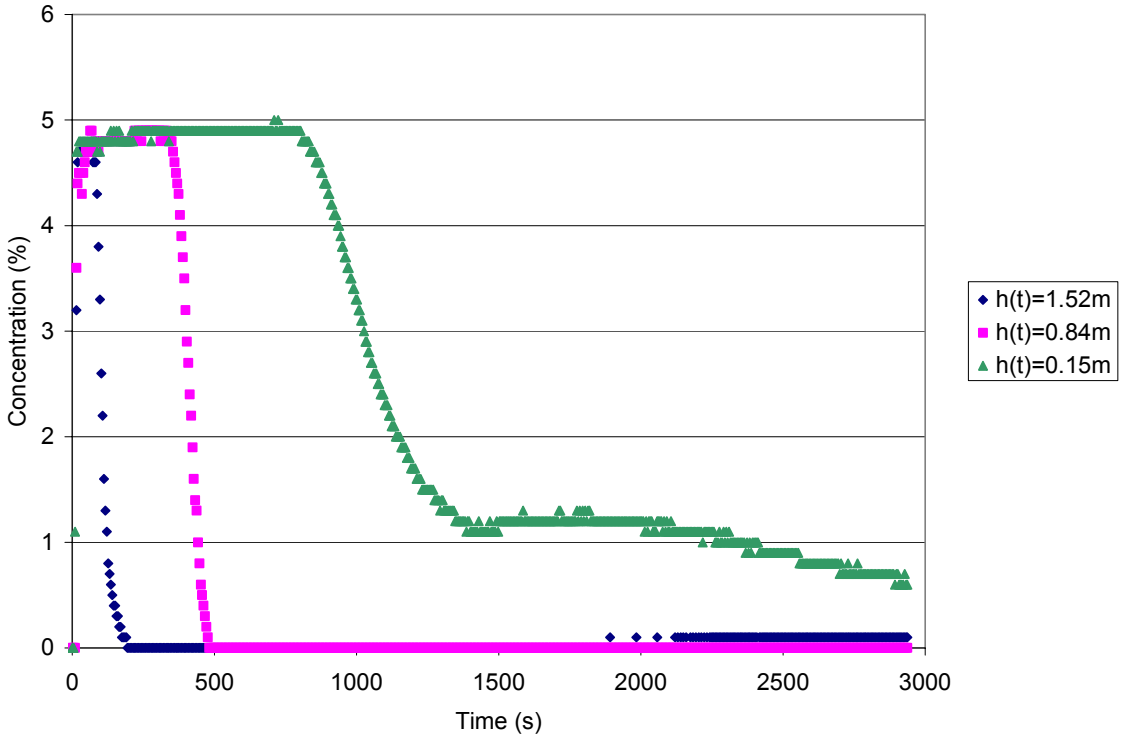

Figure 12 Time-Concentration profile, Ao=Ai=0.00038 m^2, C_o=4.7%

Based on the concentration profiles observed in these experiments, it can be assumed that the flow behavior represents that of a descending interface rather than the continuous mixing model. However, this interface is not a sharp interface. Instead of the profile appearing as a step-wise function, there exists a period of time where the concentration at a given height is decreasing. This wide-interface behavior becomes more apparent as the interface gets closer to the floor.

If the upper and lower leakage areas are equally reduced, the time-concentration profile remains similarly shaped, but the time for the interface to reach each sample elevation increases. Although the hydrostatic driving force remains the same, the area available for leakage decreases, decreasing the volumetric flowrates. Figure 13 and Figure 14 show the increased hold time for the agent to reach the respective ports as well

as a wider interface at each port. The experiment shown in Figure 13 and Figure 14 have equal upper and lower leakage areas equaling 0.000253 m^2 and 0.000127 m^2, respectively.

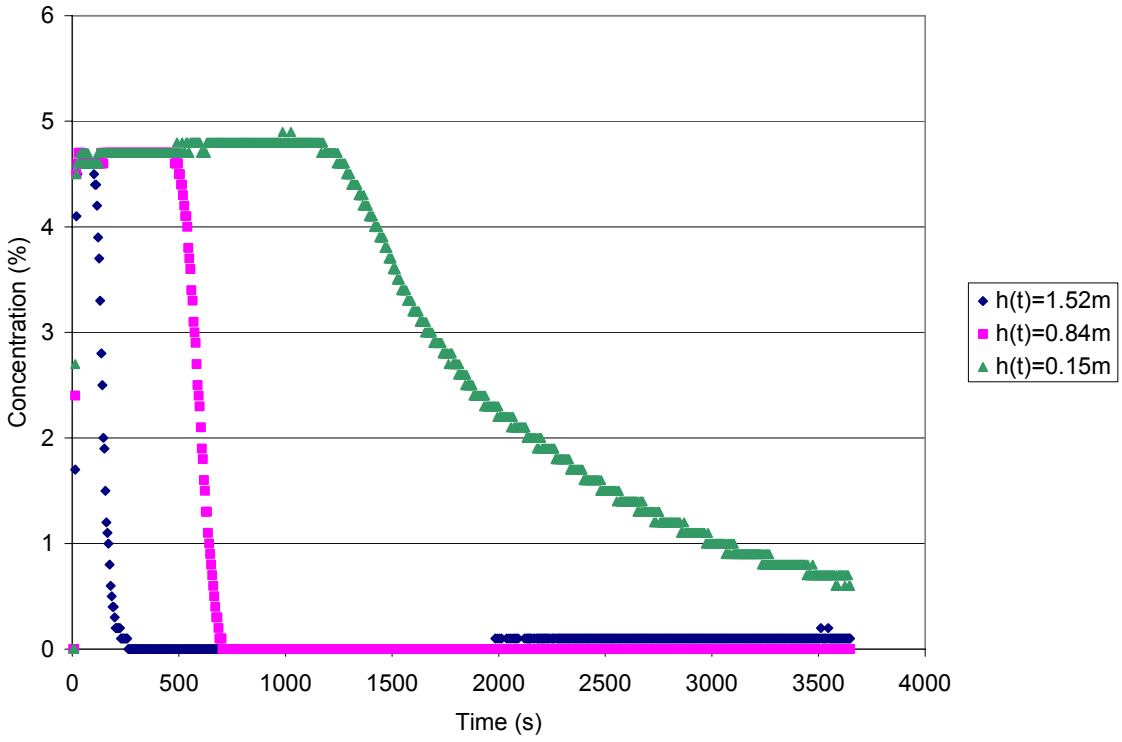

Figure 13 Time-Concentration profile, Ao=Ai=0.000253 m^2, C_o=4.7%

For the experiment with leakage areas of 0.000127 m^2, the interface descends as expected past the first two sample ports. The flow behavior at the lowest sample port shows a very wide interface height. The concentration at this height begins to drop at almost the same time the interface passes the middle sample port. The flow behavior changes from a descending interface to that of a continuous mixing model, once the interface descends half-way down the enclosure. This change in flow behavior could be due to the large amount of time it takes for the interface to reach this height as well as a reduced hydrostatic pressure differential at the bottom of the enclosure.

The hydrostatic pressure profile during a test is shown in Section 4.3 as Figure 19. After approximately 1500 seconds a negative pressure difference between the inside and outside of the enclosure develops. This negative pressure difference could allow for air to flow into the enclosure through the lower leakage holes and create mixing of the agent-air layer, reducing its concentration over time rather than remaining an actual descending interface.

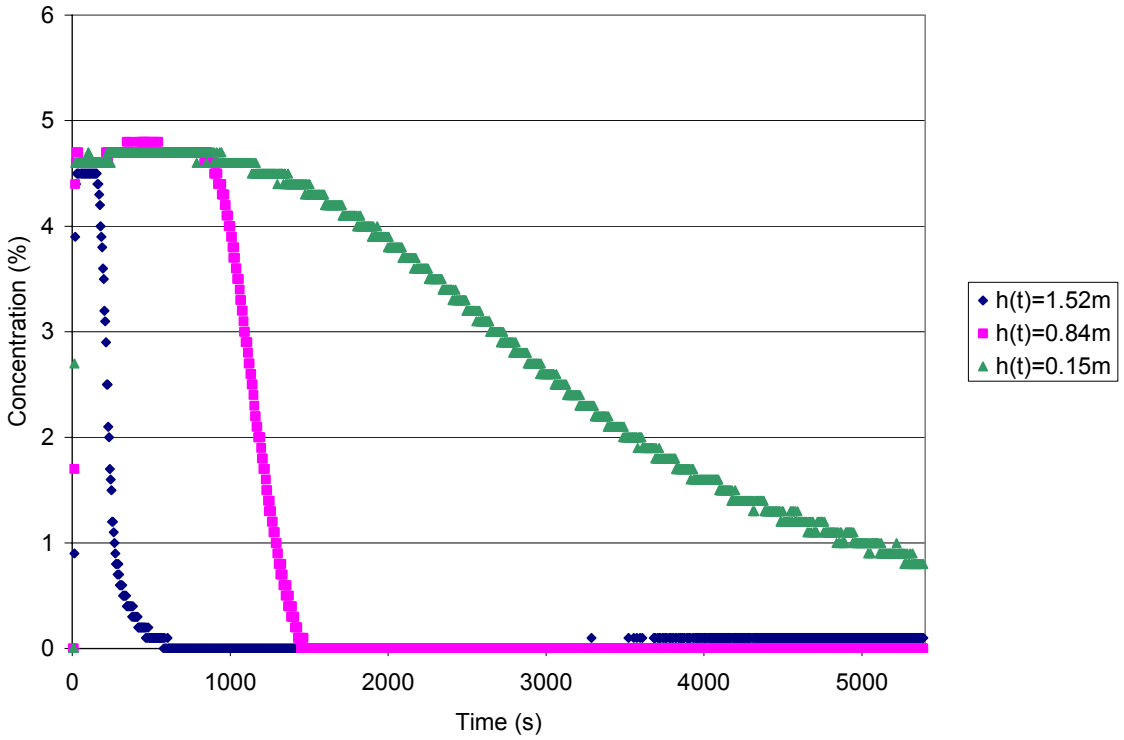

Figure 14 Time-Concentration profile, Ao=Ai=0.000127 m^2, C_o=4.7%

For the three previous cases discussed, the upper and lower leakage areas were equal. An experiment conducted with a leakage area ratio of 0.33 is shown in Figure 15. With this area ratio, the leaks available for flow essentially represent unrestricted inlet flow with restricted outlet flow. These time-concentration profiles are similar to those

seen in the equal area case; an interface is formed and the width of the interface increases as the interface descends.

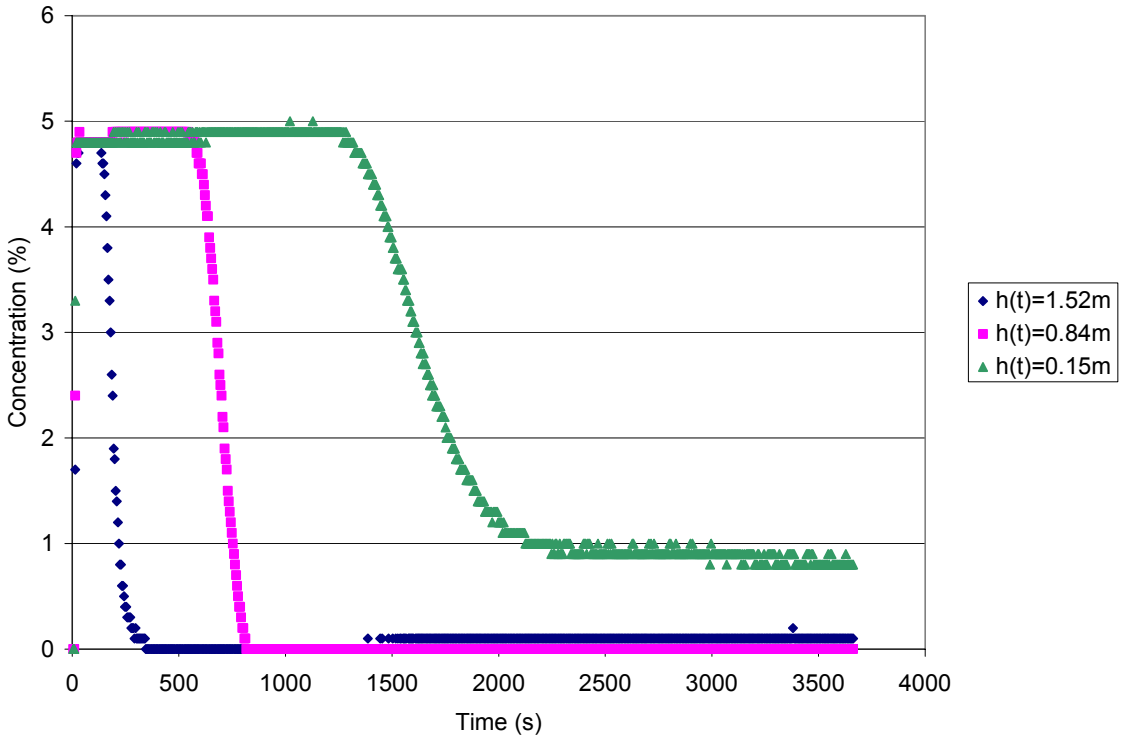

Figure 15 Time-Concentration profile, Ao=0.000127 m^2 Ai=0.00038 m^2, C_o=4.8%

Figure 16 shows an experiment with a leakage area ratio of 3. A descending interface clearly passes the first two sample ports. However, similar to the most restricted equal leakage area scenario (A_o=A_i=0.000127m^2), the lowest concentration sample port at a height of 0.22 m shows a time-concentration profile that would be expected more with the continuous mixing model than a sharp descending interface. Because of the limited inlet flow at the top of the enclosure, flow of ambient air into the enclosure could exist at the bottom leakage holes. This entrainment of ambient air for enclosures with large area ratios was predicted by Dewsbury and Whiteley (p. 261).

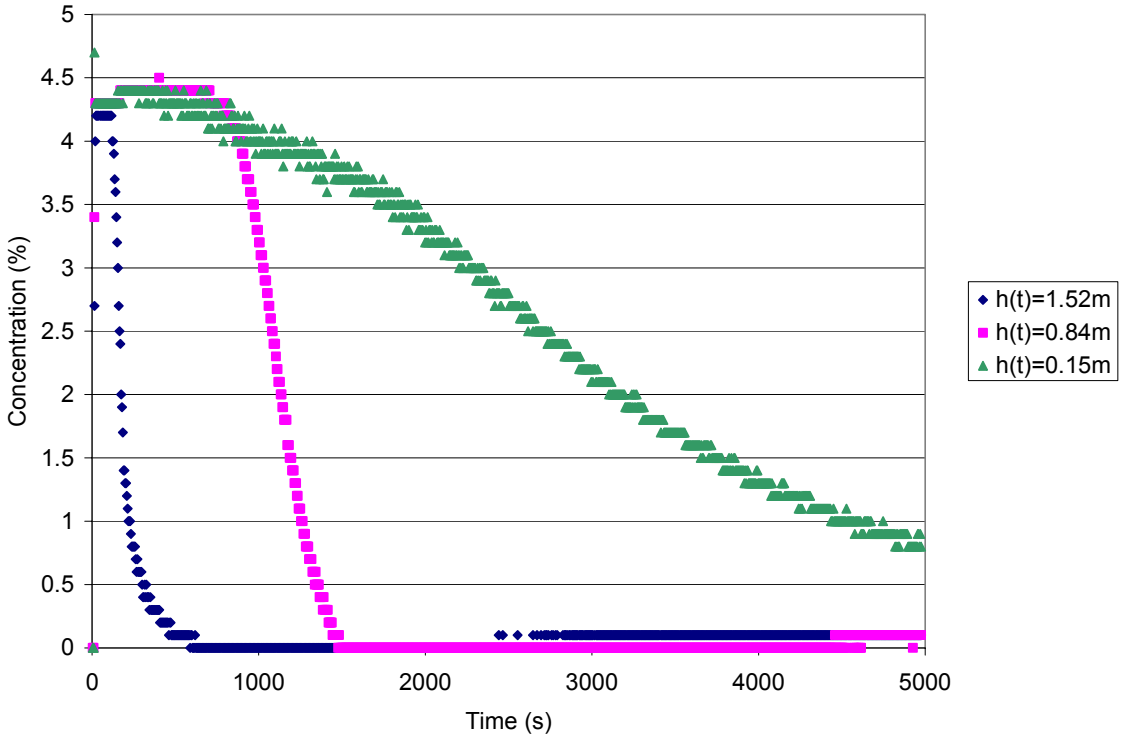

Figure 16 Time-Concentration profile, Ao=0.00038 m^2 Ai=0.000127 m^2, C_o=4.9%

4.3 Enclosure Pressure

The main driving force for flow out of the enclosure is the hydrostatic pressure created by the denser agent-air mixture. When the agent is discharged into the enclosure there is an initial decrease in the pressure while the agent is vaporizing. After this decrease in pressure, there is an increase of pressure due to an increase in volume of the agent-air mixture as it increases from the lower discharge temperature to that of the surroundings (approximately 25ºC). This transient pressure behavior for the first minute after discharge is shown in Figure 17, however these transient negative and positive pressure spikes only occur for approximately the first 15 seconds of the test.

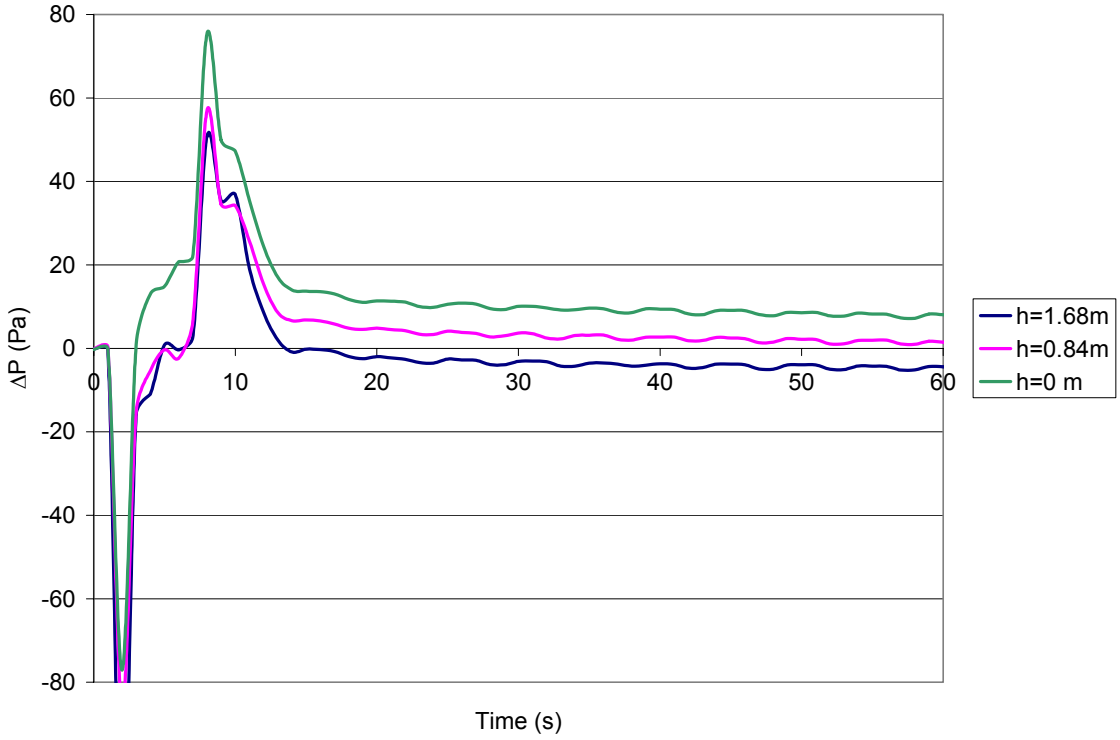

Figure 17 Initial Transient Hydrostatic Pressure Profile Ao=Ai=0.00038 m^2, C_o=4.7%

After this transient behavior, typical hydrostatic pressure profiles exist at the different heights. This behavior is shown in Figure 18. At the highest measured point (h=1.76m) there is a negative pressure difference between the enclosure pressure and the ambient air pressure. This pressure difference is responsible for the entrainment of the fresh air into the enclosure. At the lowest height (h=0.077m) there exists a positive pressure difference, forcing the agent-air mixture out of the enclosure. As the interface layer descends, these pressure differences decrease resulting in a smaller flowrate. These small pressure differences are responsible for the wide interface at the lowest sample port. The small driving force, and thus flowrate, result in the interface taking more time to pass a low height on the enclosure.

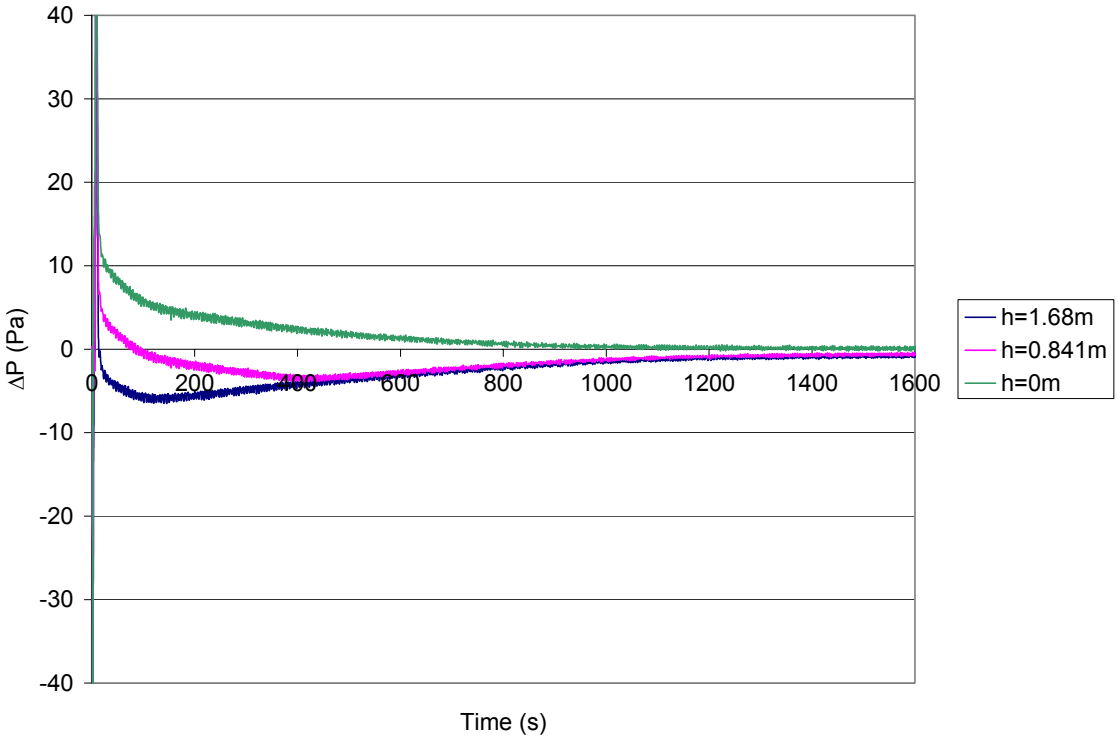

Figure 18 Hydrostatic Pressure Differences Ao=Ai=0.00038 m^2, C_o=4.7%

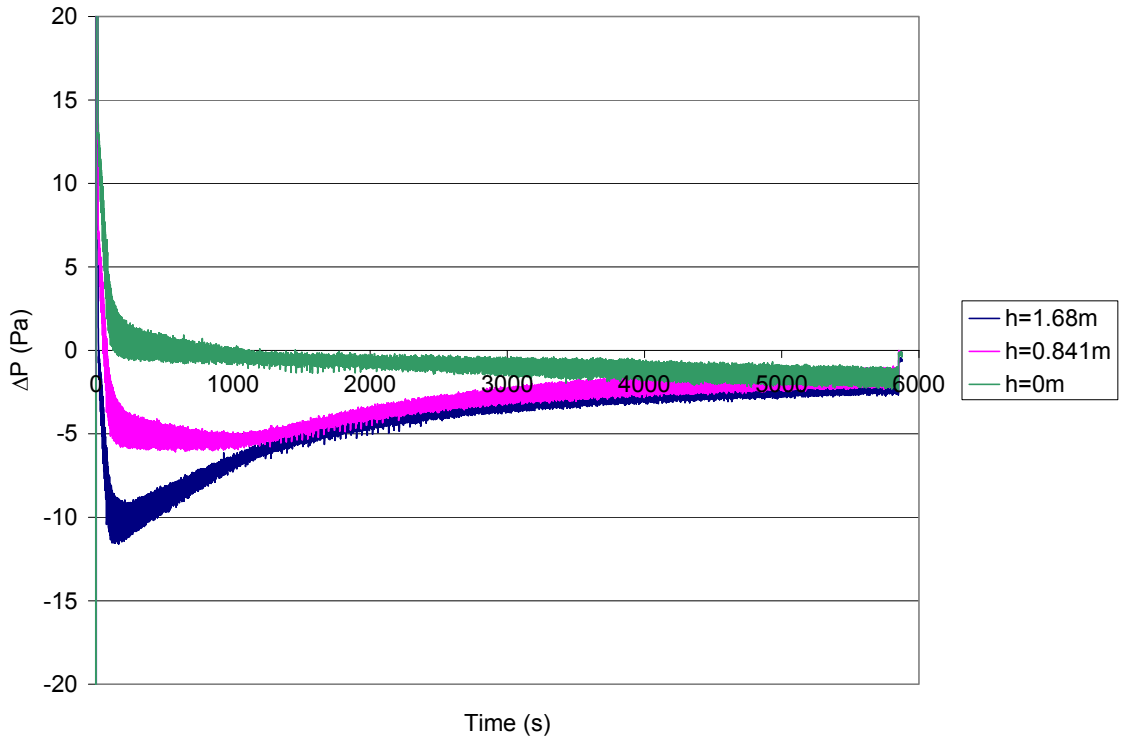

Figure 19 Hydrostatic Pressure Differences Ao=Ai=0.000127 m^2, C_o=4.7%

4.4 Dimensionless Comparison

The hold time of agent-air mixture within an enclosure is a function of the leakage area, the density of the mixture, as well as the height of the interface. These parameters will differ between experiments and enclosures. Therefore in order to best compare numerous situations, the hold time should be made dimensionless. The time-concentration data collected by the Tripoint analyzer was made dimensionless by the equations presented in Section 2.4. Therefore all data collected could be compared to the descending interface model.

Figure 20 shows the dimensionless descending interface ($h(t)/H_o$) as a function of the dimensionless quantity $k(t-t_o)/\tau$. This parameter encompasses all the experimental parameters of each test. The experimental data reported is at the point where the

concentration dropped below 80% of the initial concentration. This is referred to at the leading edge of the interface because it is the point at which the concentration was approximately 5% above the Novec 1230 minimum extinguishing concentration for Class A hazards.

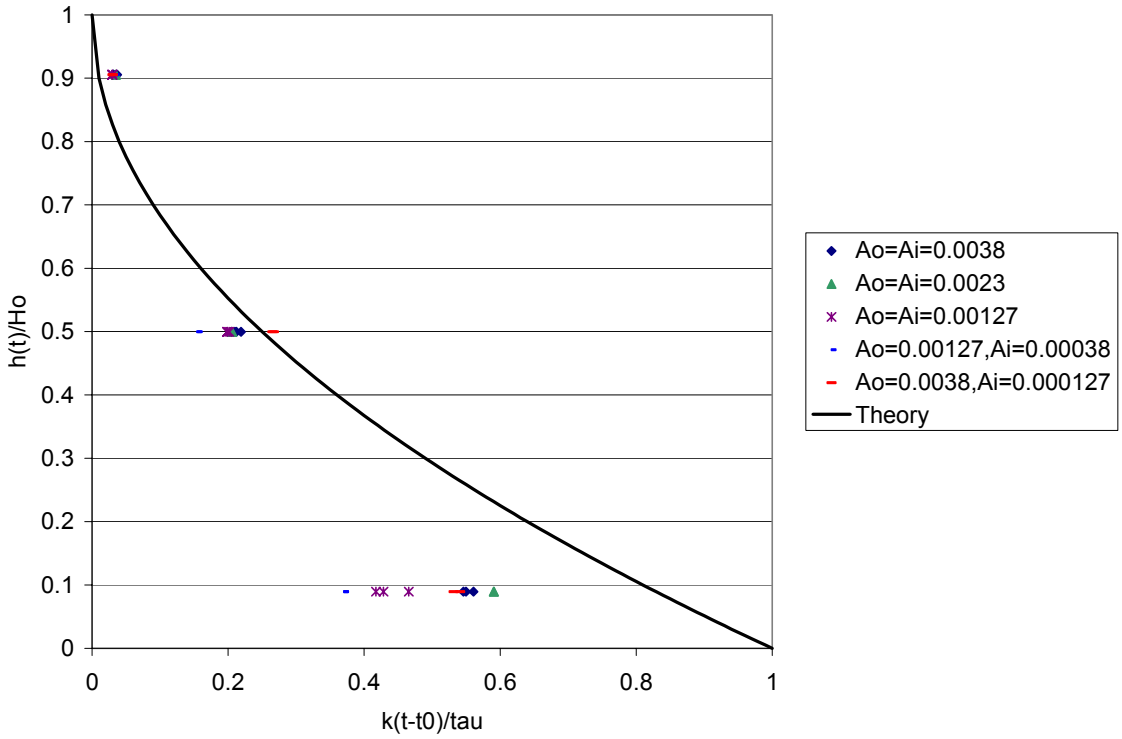

Figure 20 Dimensionless Descending Interface, Experimental data C=80%(Co)

As shown in Figure 20 the behavior of the descending interface is close to the sharp descending interface theory as it descends along the first two concentration points. The first concentration sample port is located at a height of 1.52 m. The actual interface moves slower than theoretically predicted. At the second concentration port, height of 0.84 m, the actual interface descends slightly faster than expected. The time for the concentration to reach 80% of the initial concentration is 15-18% faster than theoretically predicted. At the lowest concentration port the actual interface does not closely follow

the descending interface model at the lowest concentration port. At this bottom location the interface layer descends quicker than predicted by theory. The experimental enclosure could have additional upper leakage that is not known. This additional leakage would increase the rate of descent of the upper layer.

For comparison, the point at which the agent-air concentration reached 50% of the initial concentration was also recorded and plotted against $k(t-t_o)/\tau$. This concentration could be considered the trailing edge of the interface and resembles concentrations below the minimum extinguishing concentration of Novec 1230. Similar to the experimental data the descending interface layer moves faster than predicted by theory. The model represents the flow behavior at points greater than half of the enclosure height, but does not favorably predict the behavior when the layer descends past this height. The time for the concentration to reach 50% of the initial concentration for the sample port located at a height of 0.84 m is 8-20% faster than that predicted by theory, with the exception of the case where the lower leakage is three times that of the upper leakage. For the case where the upper leakage is greater than the lower leakage, the layer descends slower than predicted by theory.

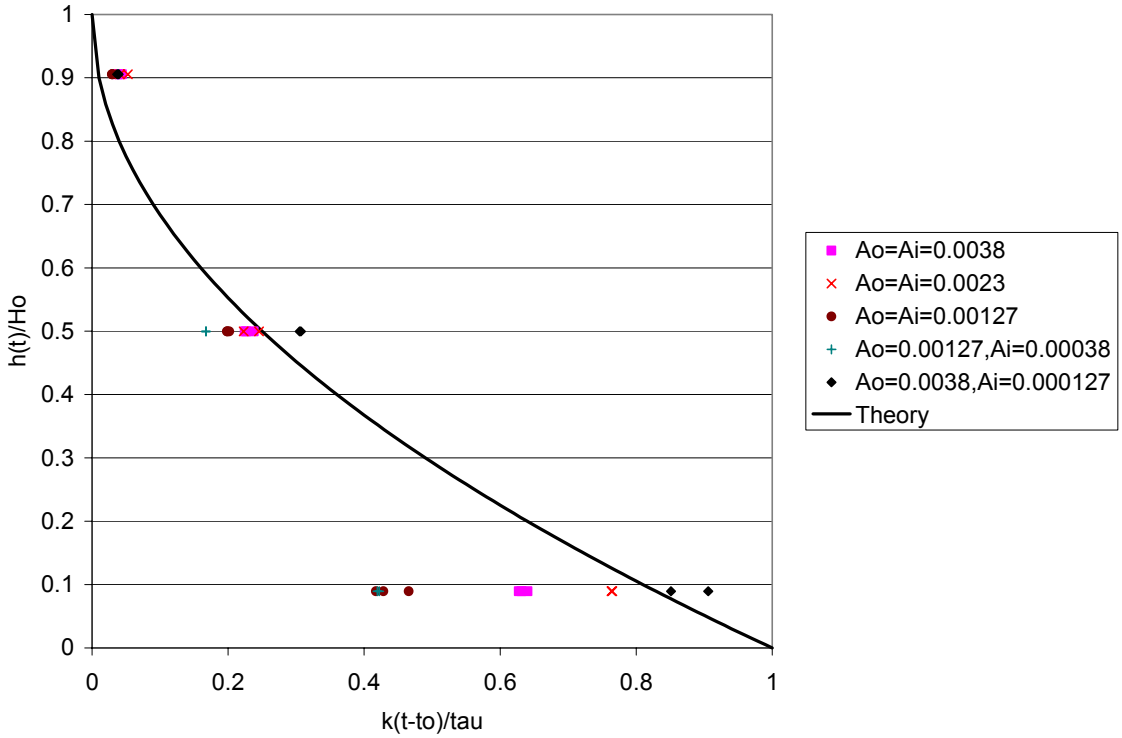

Figure 21 Dimensionless Descending Interface Experimental data @ C=50%(Co)

The effect of the area ratios is also seen in these dimensionless graphs. The data for the hold time at the uppermost port is clustered. At the middle port the experiments with equal area are clustered while those with either restricted or increased outward flow seem like outliers. At the bottom sample port the experimental data for a given area ratio is clustered, but does not show similarity between experiments. Again, this lack of similarity between experiments could be due to bidirectional flow once the descending interface reaches heights less than half of its initial height.

Chapter 5: Summary and Conclusions

The main objective of this study was to evaluate the descending interface model of the flow of fire suppression agent-air mixtures out of an enclosure. Fifteen experiments were conducted using Novec 1230 and different leakage area scenarios. The descending interface model proved to correctly predict the descent of the layer over the upper half of the height of the enclosure. Below this, model under predicted the amount of time it took for the layer to descend to a height of 0.15 m from the lower leakage opening. The reason for the under-prediction of the hold time could be due to the possible change in interface behavior from a sharp descending interface to a wide interface or continuous mixing model.

Based on this investigation, the descending interface model adequately predicts hold times to a height of approximately one-half that of the initial interface height for agents with similar characteristics to Novec 1230. As long as the highest potential fire source within the enclosure is in the lower half of the enclosure and the hold time is considered the point where the interface drops to this point as stated in the NFPA 2001 standard, this model appears to be suitable for design purposes.

Further experiments with agents of different densities are needed to further validate the descending interface model, as well as determine the agents for which this model is valid. More concentration-time data gathered at the lower half of an enclosure would help to better characterize the flow and interface characteristics at these heights.

The agent discharge causes negative and positive surges in internal enclosure pressure. In order for the suppression to be effective, the enclosure needs to be able to

withstand these pressure surges. Further analysis of these transient pressure effects is warranted.

.

Appendix A: Raw Data and Supplemental Graphs

A total of 13 experiments were run with five different leakage area conditions. Table A-1 outlines the experiment name, leakage areas, initial concentration, densities, and the calculated parameters k_2 and t used in the dimensionless comparison.

Table A-1 Experimental Raw Data

Experiment	Ao (m2)	Ai (m2)	Co (%)	ρo (kg/m3)	ρm (kg/m3)	k2	τ	t(Ho/2)pre (s)
072805_Test2	0.00038	0.00038	5.5	0.168	1.855	0.337	521.48	453.24
080105_Test1	0.00038	0.00038	4.6	0.168	1.742	0.314	521.48	486.30
080305_Test1	0.00038	0.00038	4.7	1.168	1.755	0.317	521.48	482.13
080305_Test2	0.000253	0.000253	4.7	1.168	1.755	0.317	782.22	723.19
080305_Test6	0.000253	0.000253	4.75	1.168	1.761	0.318	782.22	720.14
080305_Test3	0.000127	0.000127	4.8	1.168	1.767	0.319	1564.44	1434.29
080305_Test5	0.000127	0.000127	4.6	1.168	1.742	0.314	1564.44	1458.89
080505_Test1	0.000127	0.000127	4.7	1.168	1.755	0.317	1564.44	1446.38
080505_Test3	0.000127	0.000127	4.75	1.168	1.761	0.318	1564.44	1440.28
080405_Test2	0.000127	0.00038	4.8	1.168	1.767	0.397	1564.44	1153.04
080405_Test3	0.000127	0.00038	4.8	1.168	1.767	0.397	1564.44	1153.04
080405_Test4	0.00038	0.000127	4.3	1.168	1.705	0.148	521.48	1030.54
080405_Test5	0.00038	0.000127	4.9	1.168	1.780	0.158	521.48	968.34

The Tripoint Analyzer gathered concentration data at heights of 1.52, 0.841, and 0.151 m. The time at which the concentration at the sample height reached 80, 20, and 50% of the initial concentration was recorded and is reported in Table A-2. For these data, time zero is the time at which discharge began.

Table A-2 Interface concentration-time data collected by Tripoint Analyzer.

Ao=Ai=0.00038 Time for concentration to reach					
Experiment	h(t)	80% (Co)	50% (Co)	20% (Co)	Δt
072805_Test2	1.52	102	113	136	34
	0.841	384	413	452	68
	0.151	290	1016	1260	970
080105_Test1	1.52	97	112	126	29
	0.841	394	418	457	63
	0.151	958	1094	1464	506
080305_Test1	1.52	97	107	126	29
	0.841	394	418	447	53
	0.151	968	1099	2417	1449
Ao=Ai=0.000253 Time for concentration to reach					
	h(t)	80% (Co)	50% (Co)	20% (Co)	Δt
080305_Test2	1.52	131	175	44	146
	0.841	554	651	97	603
	0.151	1503	3108	1605	1931
080305_test6	1.52	131	146	185	1931
	0.841	550	593	647	1931
	0.151	1498	1926	3239	1931
Ao=Ai=0.000127 Time for concentration to reach					
Experiment	h(t)	80% (Co)	50% (Co)	20% (Co)	Δt
080305_Test3	1.52	190	219	316	126
	0.841	1017	1143	1299	282
	0.151	2325	3424	5715	3390
080305_Test5	1.52	195	229	272	77
	0.841	1036	1153	1308	272
	0.151	2179	3307	5326	3147
080305_Test1	1.52	190	219	277	87
	0.841	1041	1167	1313	272
	0.151	2106	3191	4995	2889
Ao=0.000127, Ai=0.00038 Time for concentration to reach					
Experiment	h(t)	80% (Co)	50% (Co)	20% (Co)	Δt
080405_Test2	1.52	170	195	224	54
	0.841	652	705	759	107
	0.151	1503	1707	2340	837
080405_Test3	1.52	175	195	229	54
	0.841	657	705	764	107
	0.151	1503	1697	2471	968

Ao=0.00038, Ai=0.000127 Time for concentration to reach					
Experiment	h(t)	80% (Co)	50% (Co)	20% (Co)	Δt
080405_Test4	1.52	151	175	238	87
	0.841	978	119	1284	306
	0.151	1916	3040	4898	2982
080405_Test5	1.52	146	175	263	117
	0.841	929	1060	1206	277
	0.151	1834	3040	4835	3001

The following graphs show the hydrostatic pressure profiles as well as the time-concentration profiles for all experiments. The pressure data was collected at h(t) heights 1.68, .841, and 0 m and the concentration data was collected at h(t) heights of 1.52, 0.84, and 0.15 m respectively.

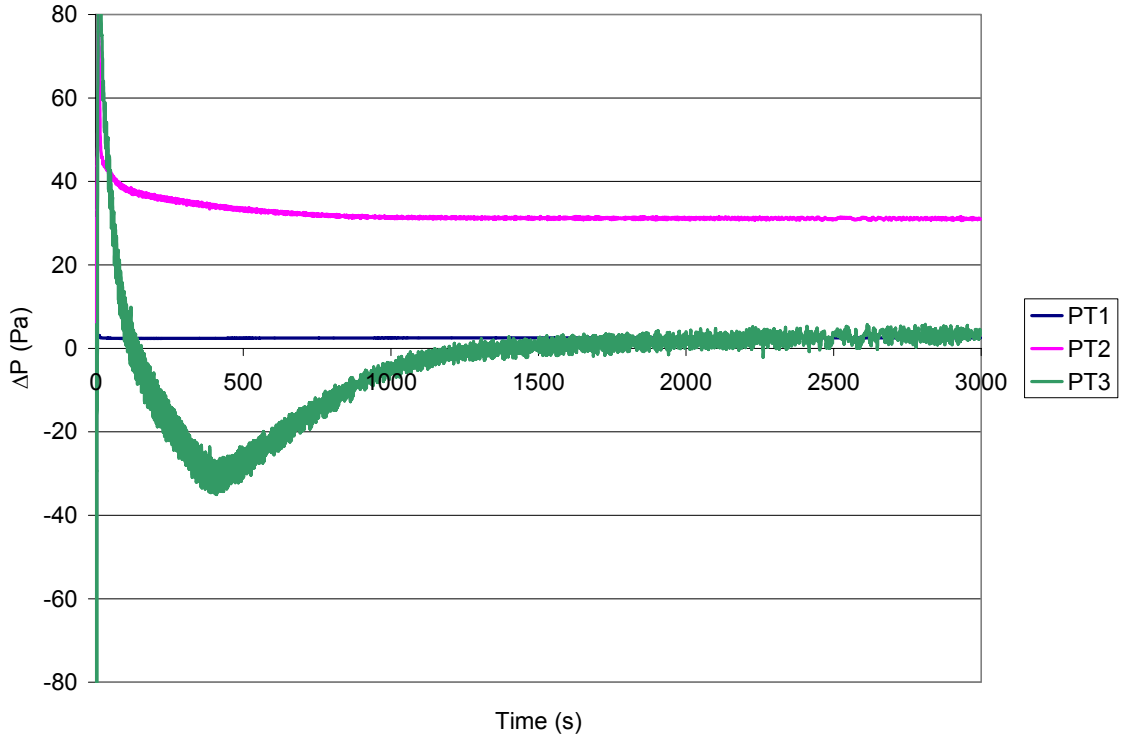

Figure A 1:Experiment 072805_Test 2 Pressure Profiles $A_o=A_i=0.00038$ m^2

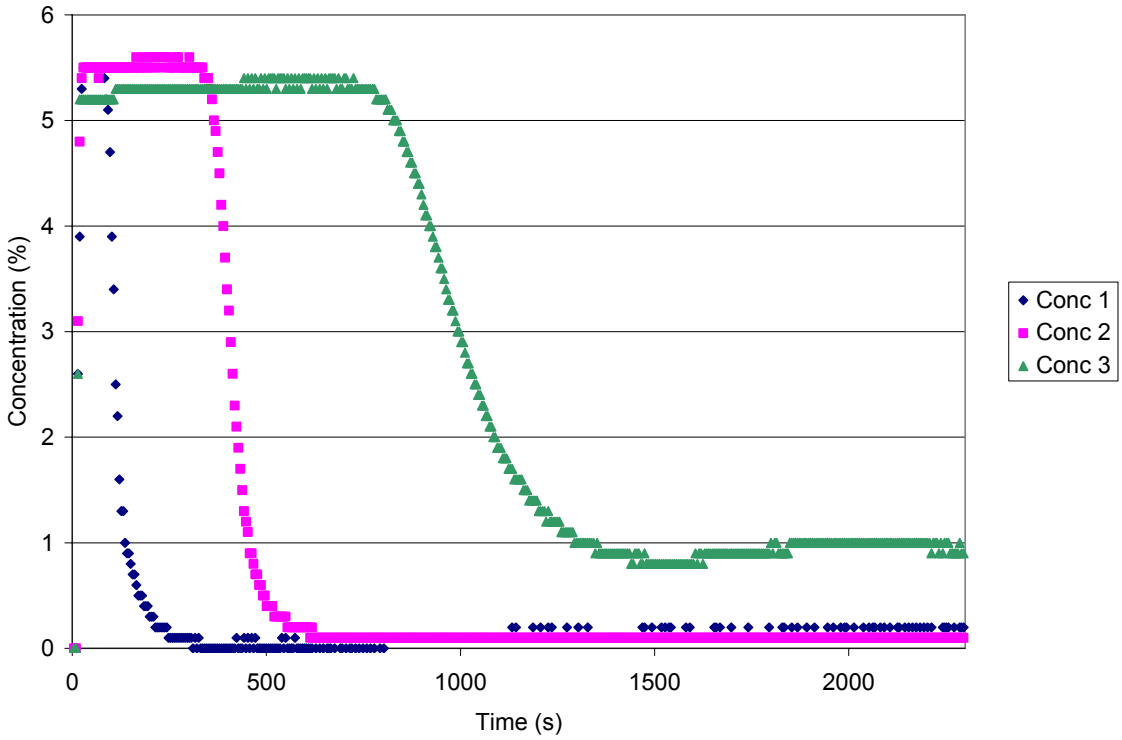

Figure A 2: Experiment 072805_Test 2 Concentration Profiles $A_o=A_i=0.00038$ m^2

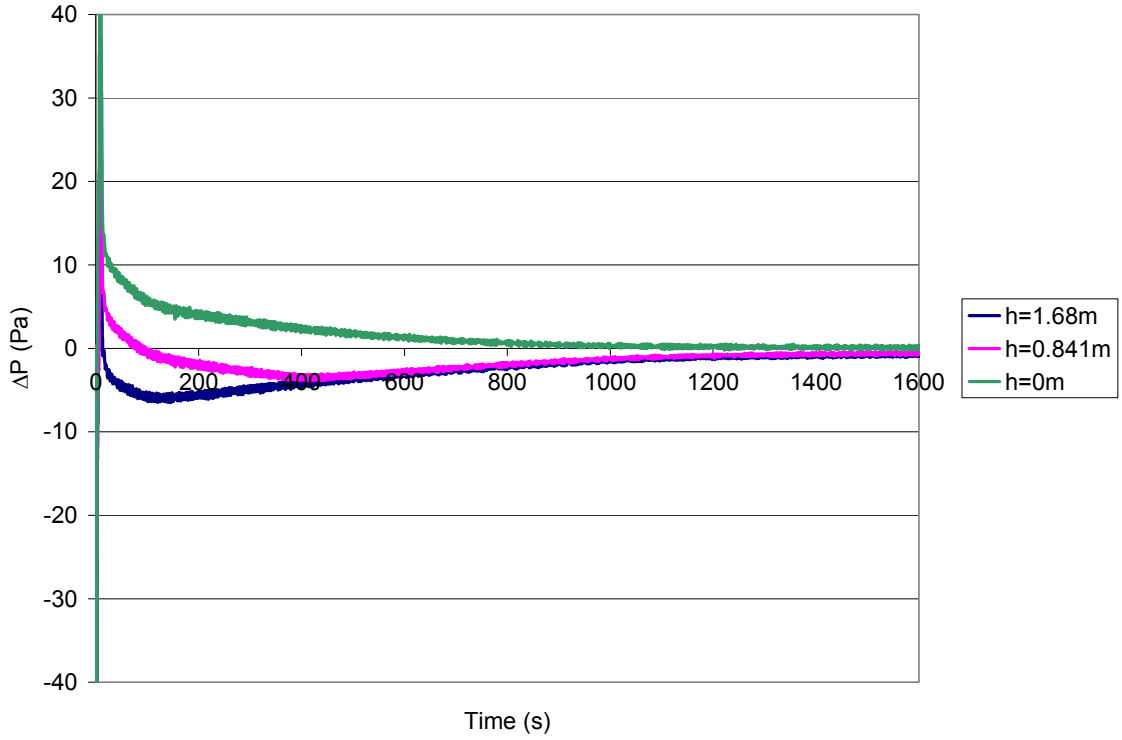

Figure A 3: Experiment 080105_Test1 Pressure Profiles $A_o=A_i=0.00038$ m^2

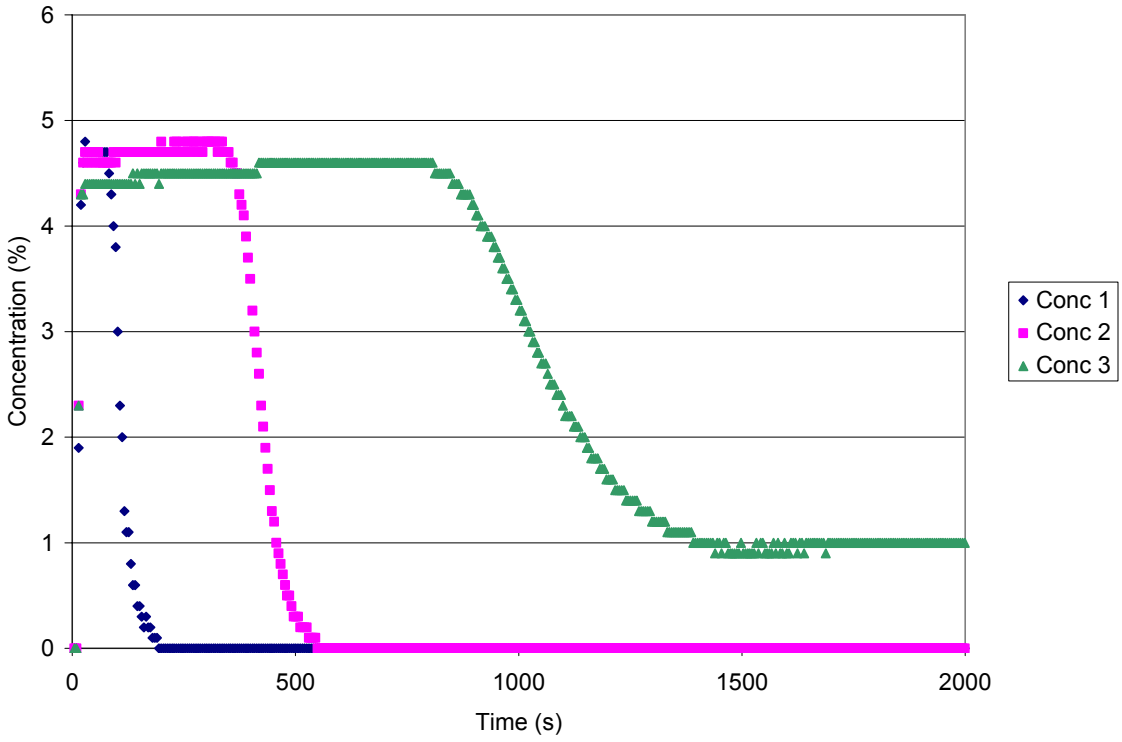

Figure A 4 Experiment 080105_Test1 Concentration Profiles $A_o=A_i=0.00038$ m^2

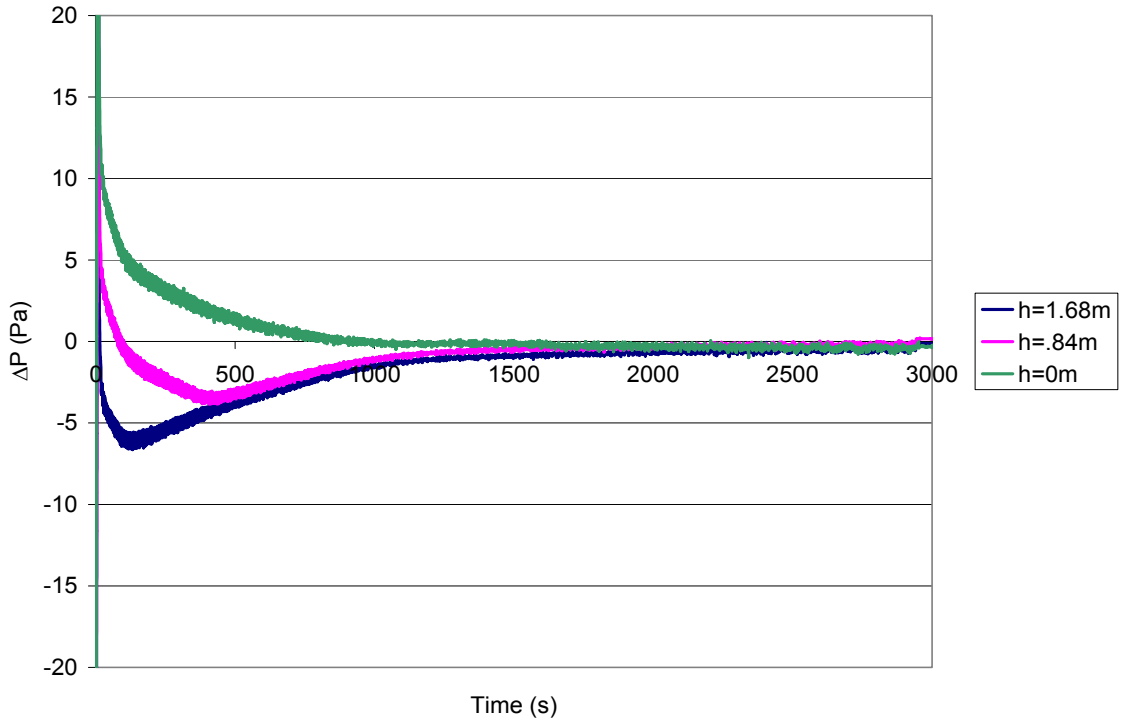

Figure A 5 Experiment 080305_Test1 Pressure Profiles $A_o=A_i=0.00038$ m^2

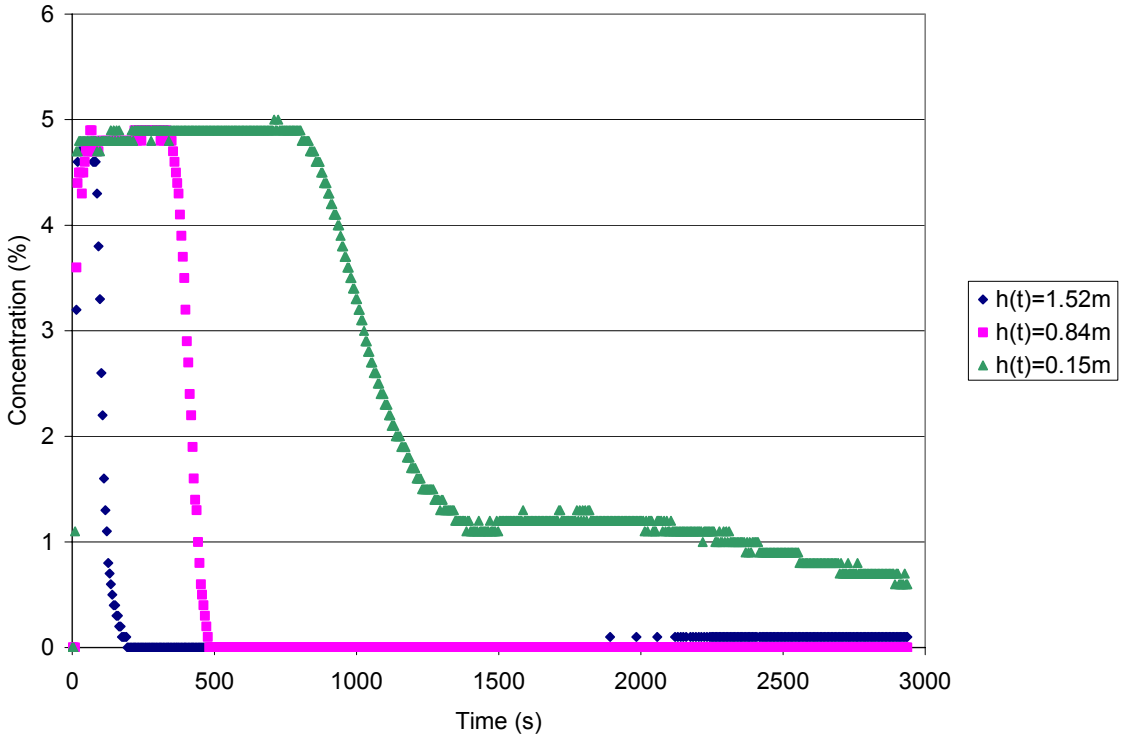

Figure A 6 Experiment 080305_Test1 Concentration Profiles $A_o=A_i=0.00038$ m^2

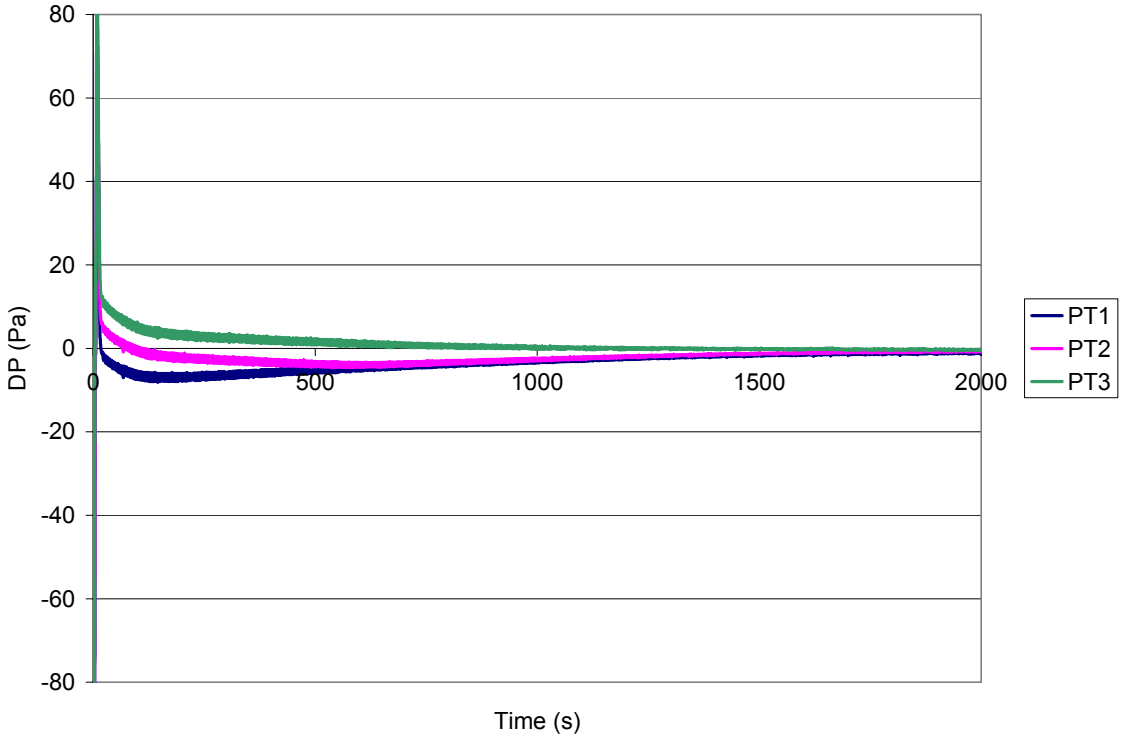

Figure A 7 Experiment 080305_Test2 Pressure Profiles $A_o=A_i=0.000253$ m^2

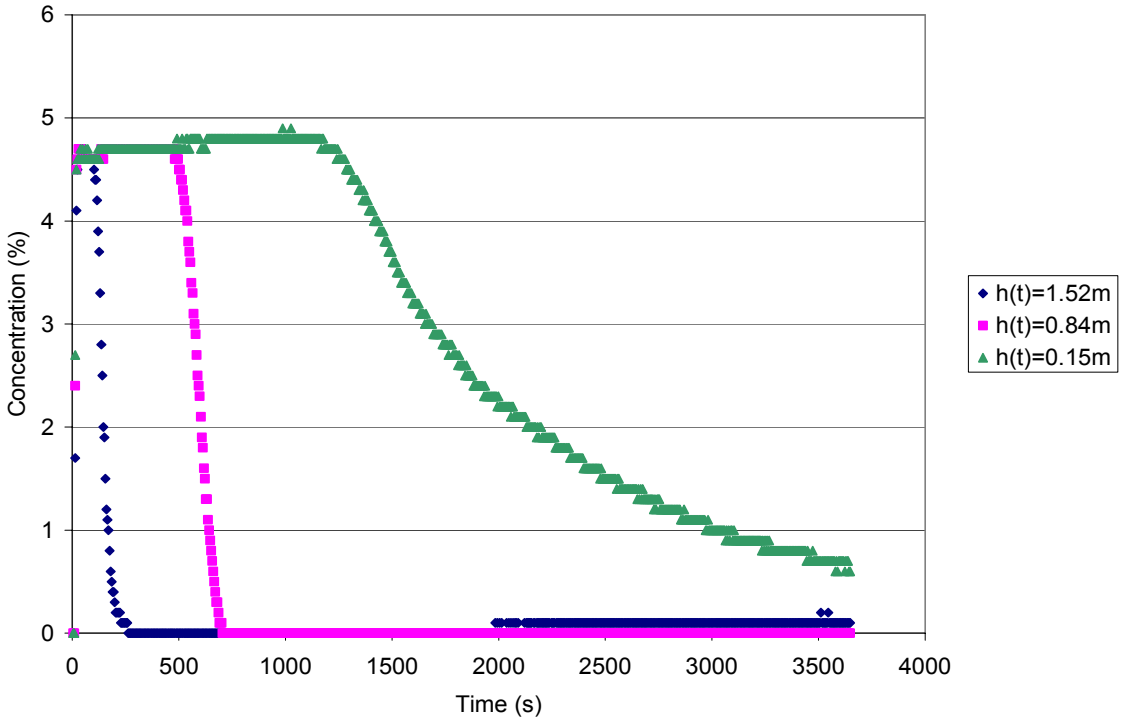

Figure A 8 Experiment 080305_Test1 Concentration Profiles $A_o=A_i=0.000253$ m^2

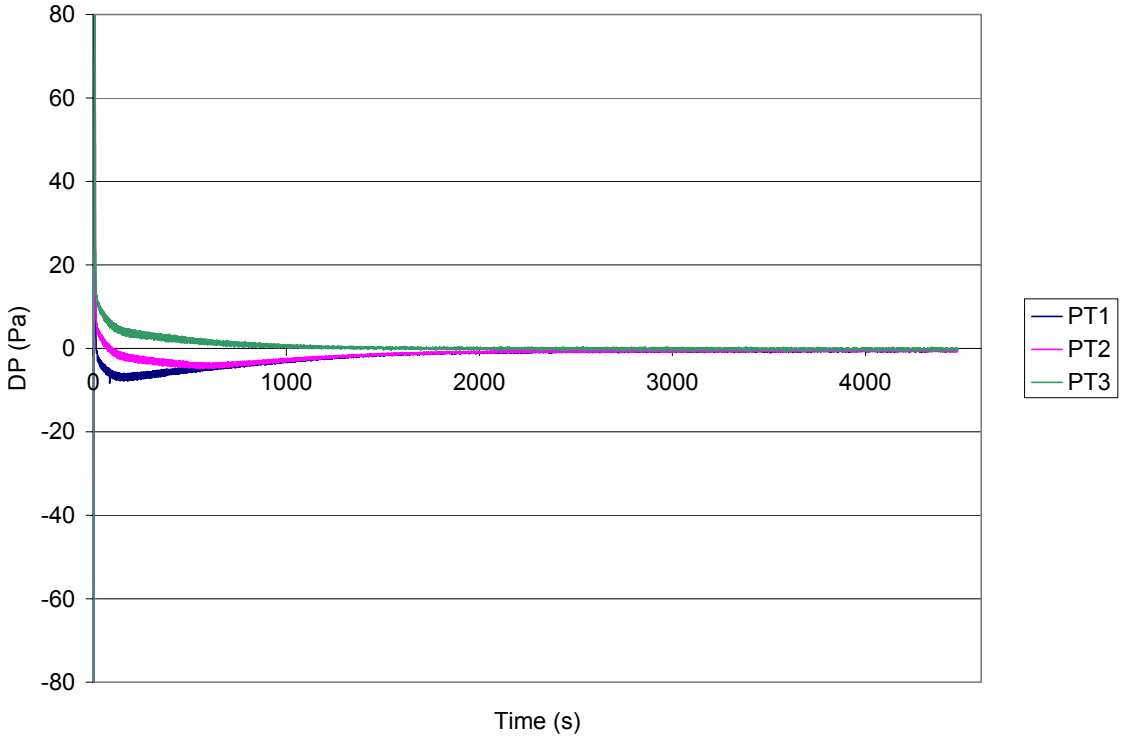

Figure A 9 Experiment 080305_Test6 Pressure Profiles $A_o=A_i=0.000235$ m^2

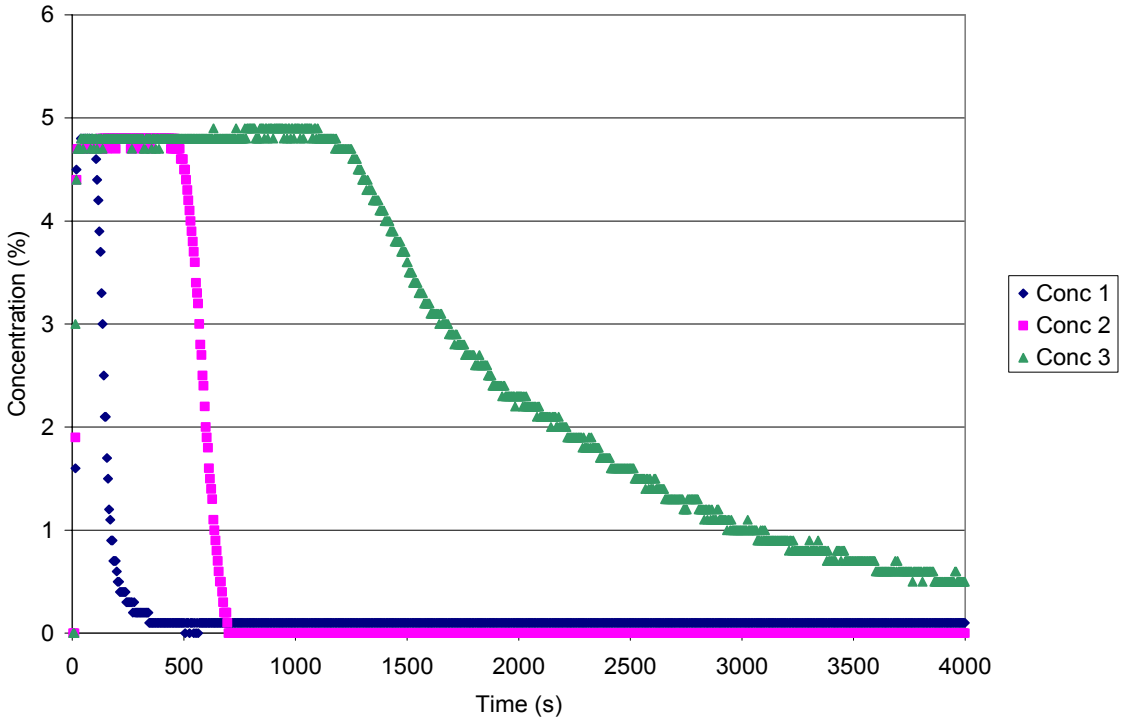

Figure A 10 Experiment 080305_Test1 Concentration Profiles $A_o=A_i=0.000235$ m^2

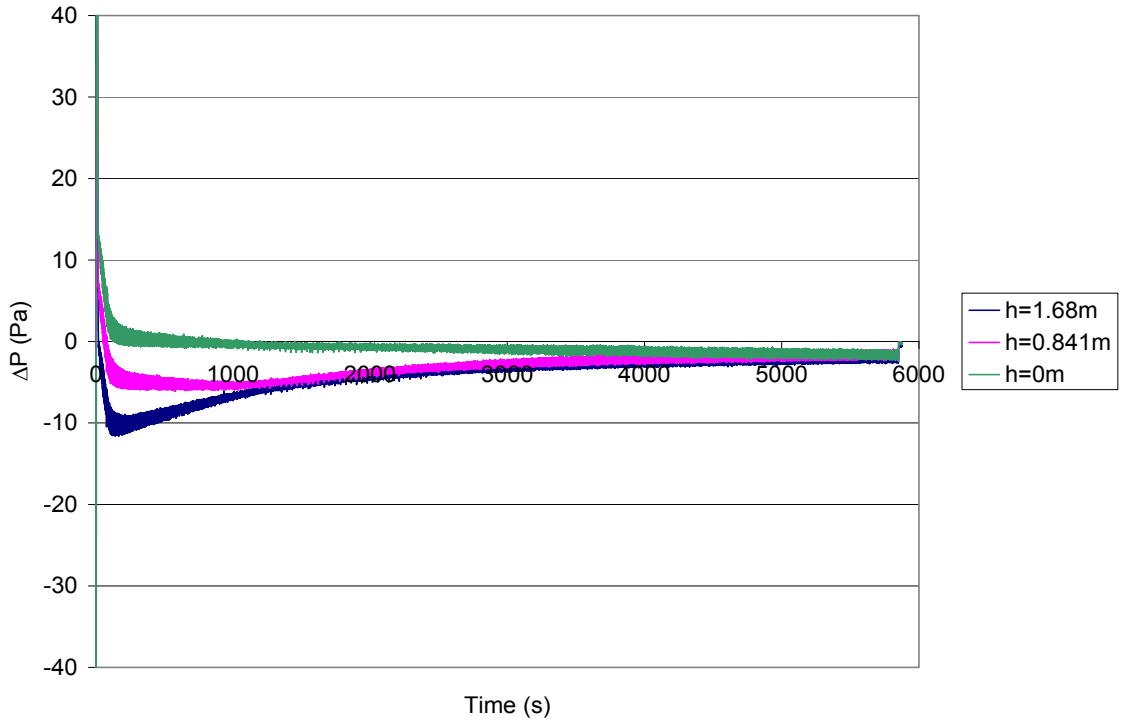

Figure A 11 Experiment 080305_Test3 Pressure Profiles $A_o=A_i=0.000127\ m^2$

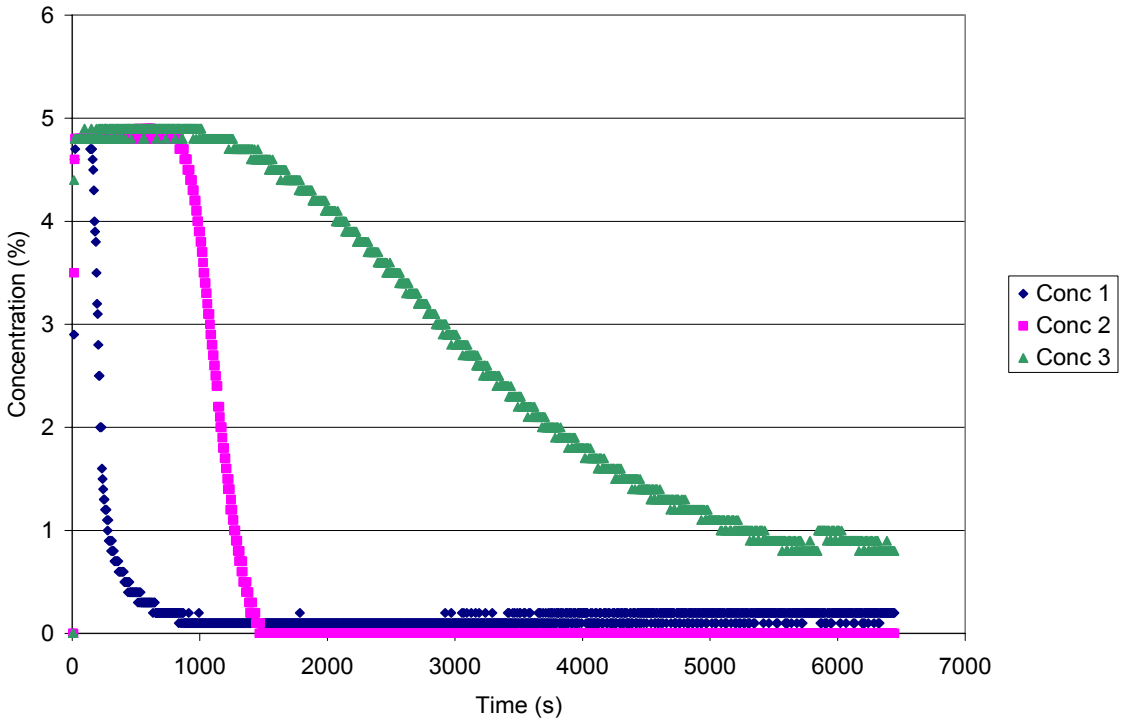

Figure A 12 Experiment 080305_Test3 Concentration Profiles $A_o=A_i=0.000127\ m^2$

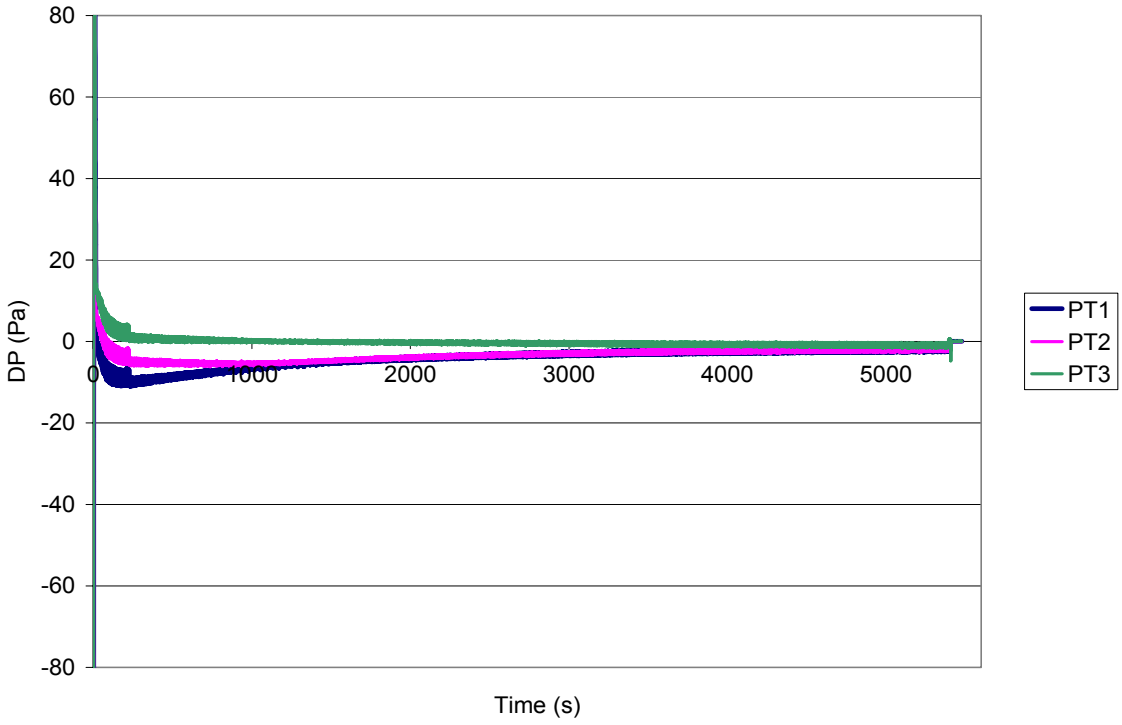

Figure A 13 Experiment 080305_Test5 Pressure Profiles $A_o=A_i=0.000127\ m^2$

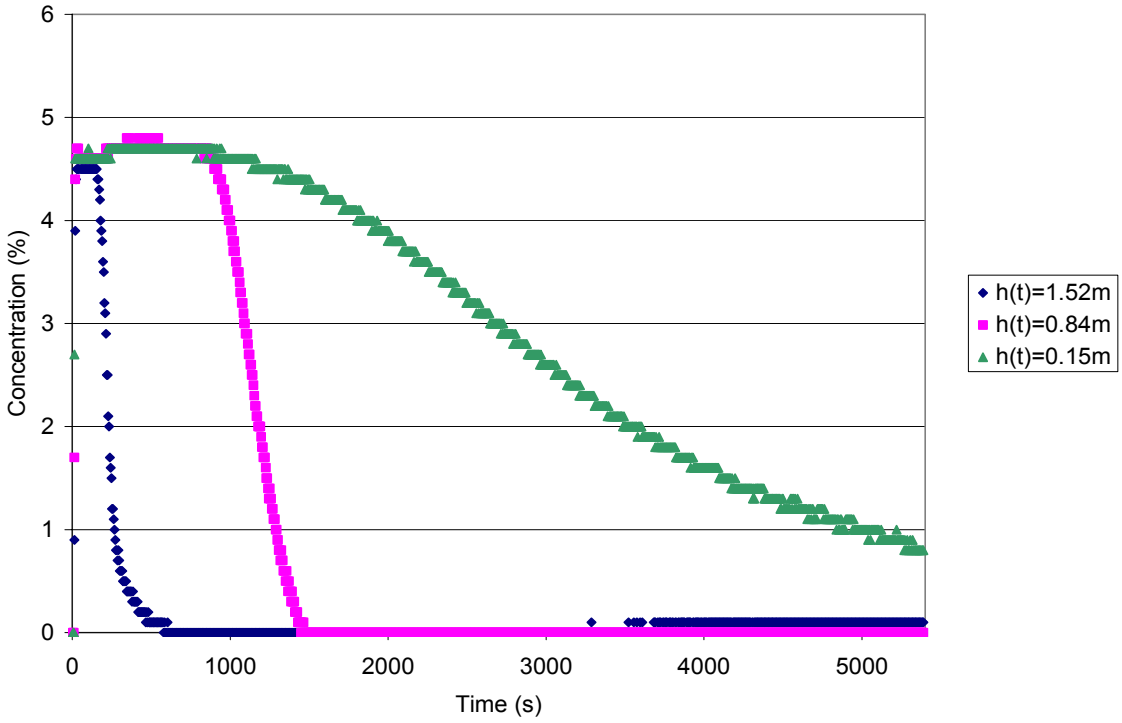

Figure A 14 Experiment 080305_Test5 Concentration Profiles $A_o=A_i=0.00038\ m^2$

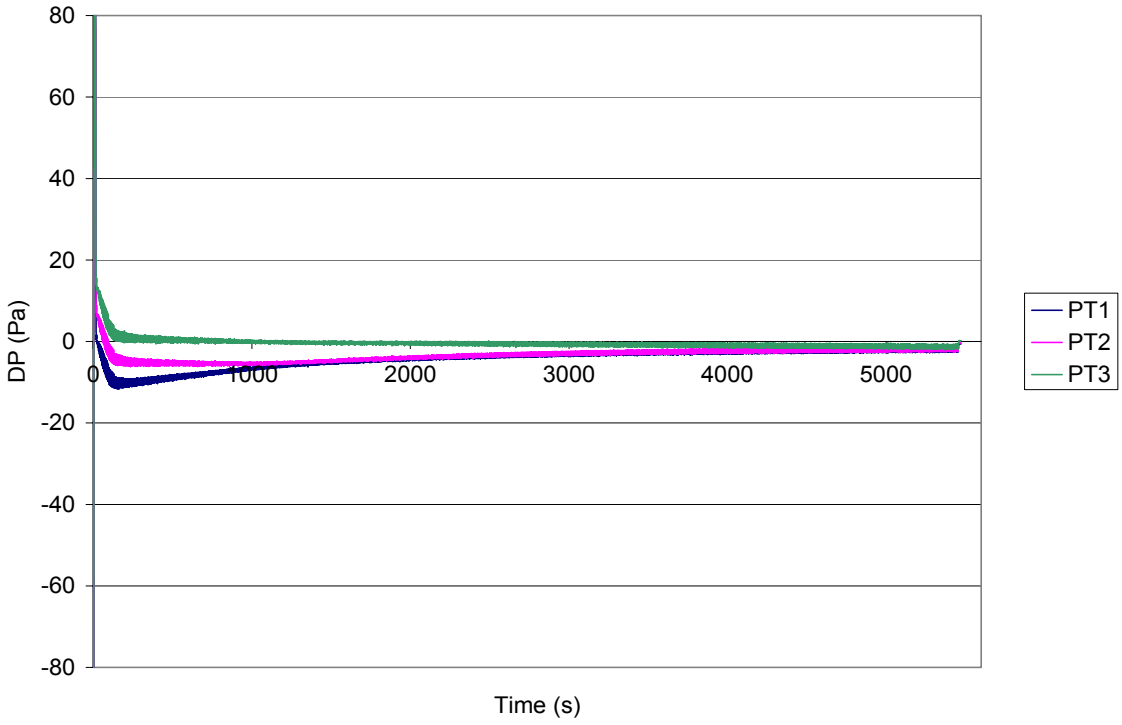

Figure A 15 Experiment 080505_Test1 Pressure Profiles $A_o=A_i=0.000127$ m^2

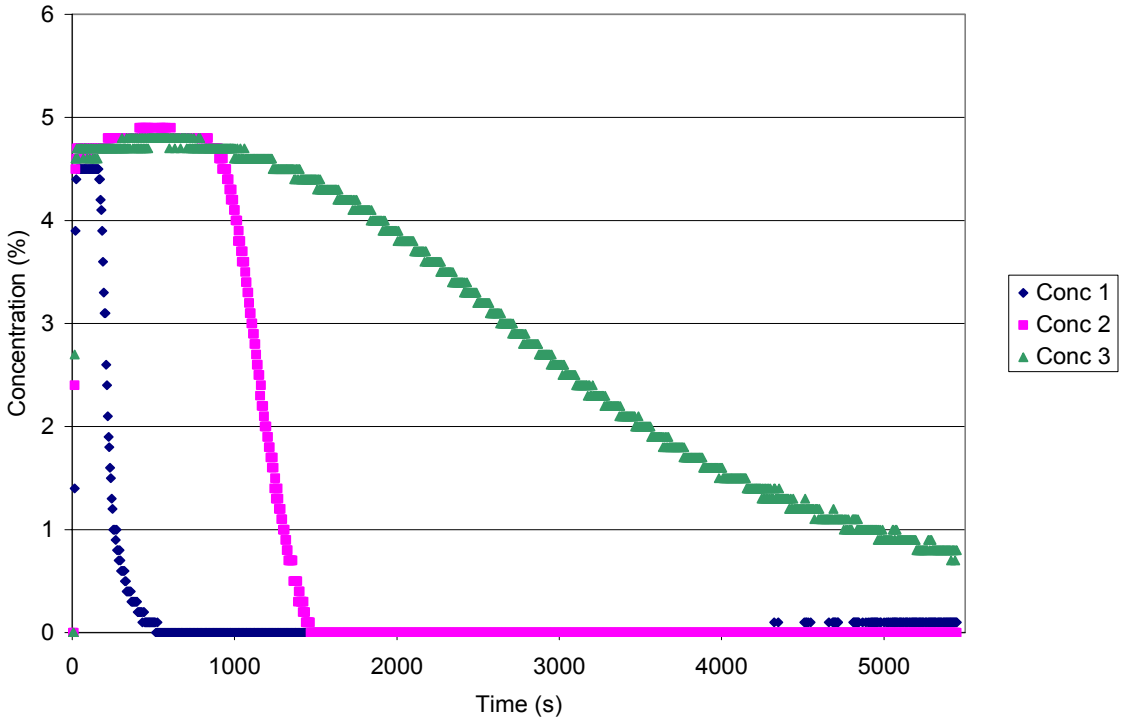

Figure A 16 Experiment 080505_Test1 Concentration Profiles $A_o=A_i=0.000127$ m^2

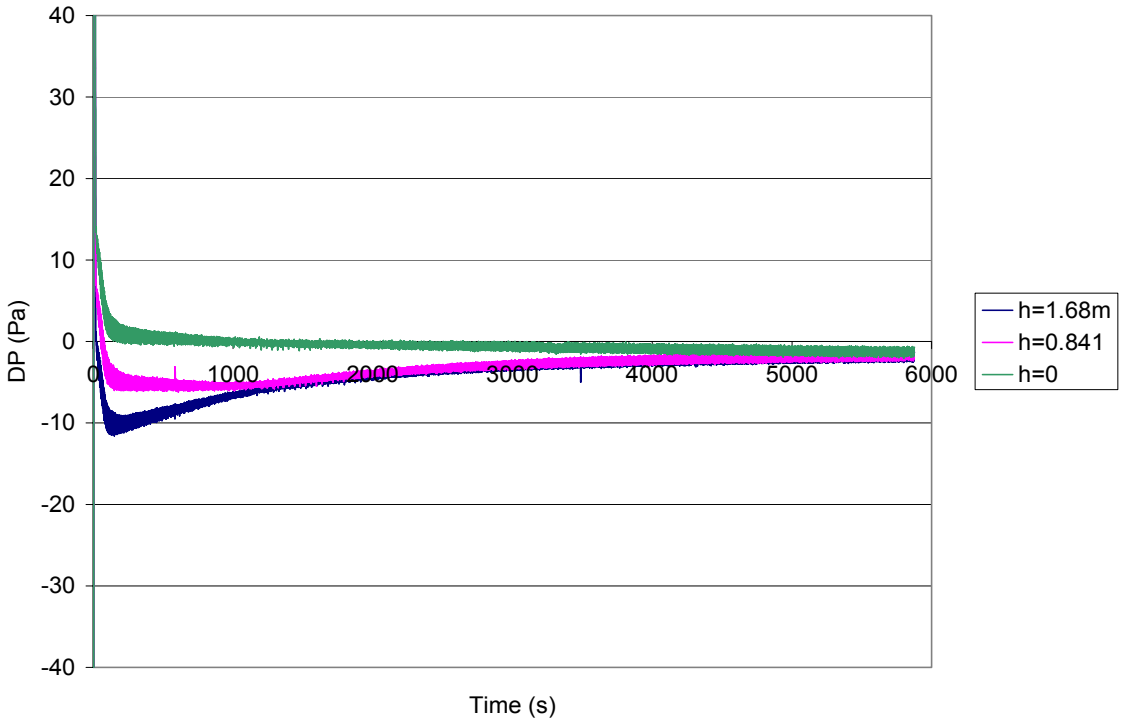

Figure A 17 Experiment 080505_Test3 Pressure Profiles $A_o=A_i=0.000127$ m^2

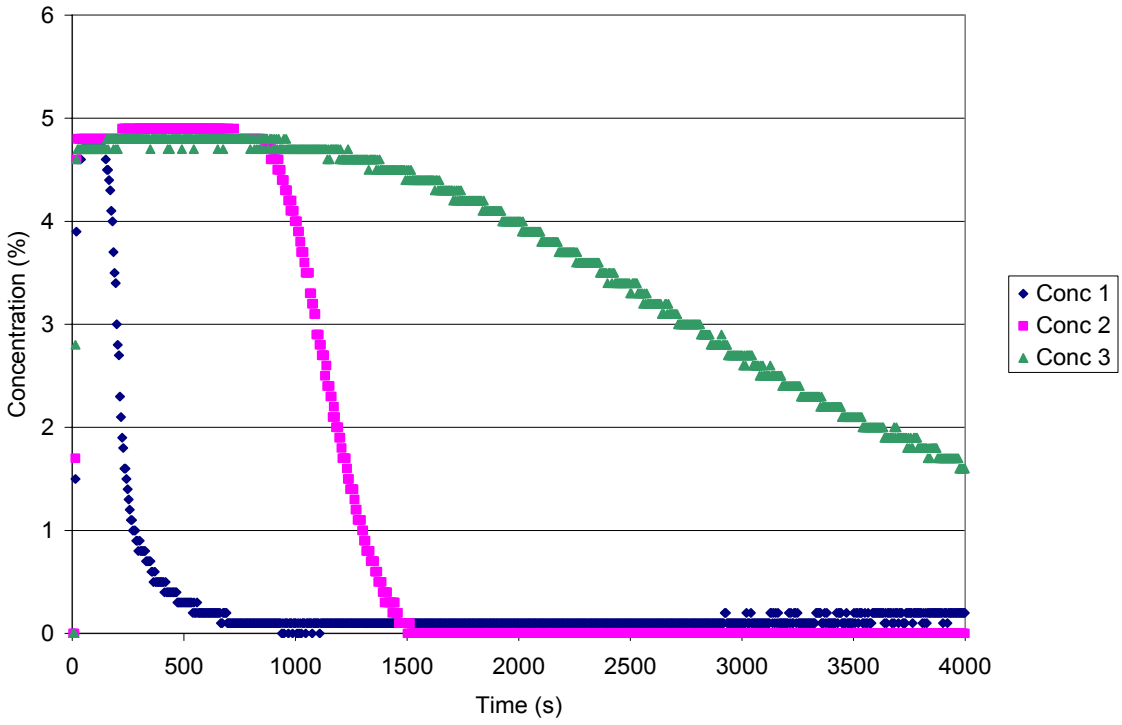

Figure A 18 Experiment 080505_Test3 Concentration Profiles $A_o=A_i=0.000127$ m^2

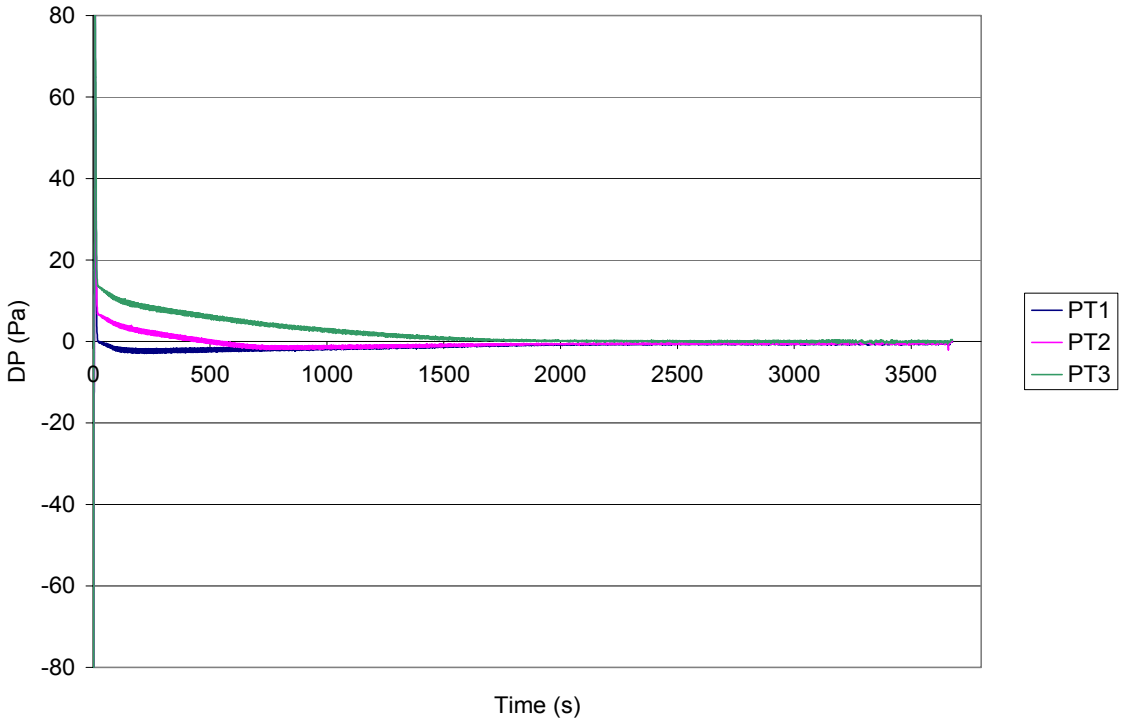

Figure A 19 Experiment 080405_Test2 Pressure Profiles A_o=0.000127 m^2 A_i=0.00038 m^2

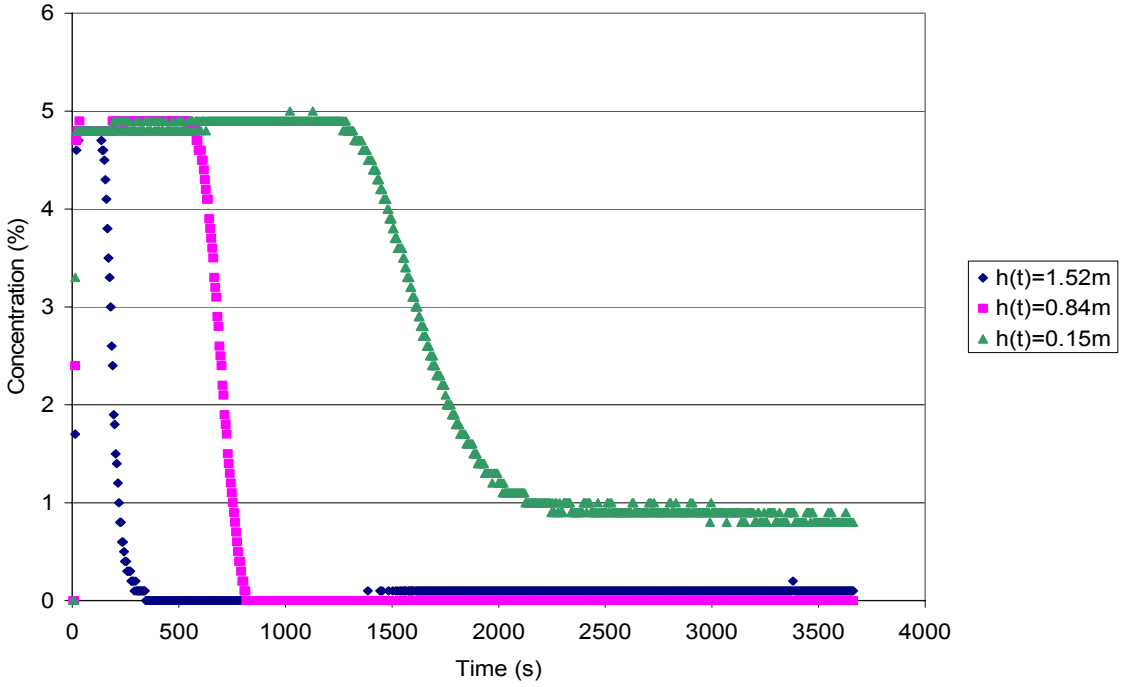

Figure A 20 Experiment 080405_Test2 Pressure Profiles A_o=0.000127 m^2 A_i=0.00038 m^2

:

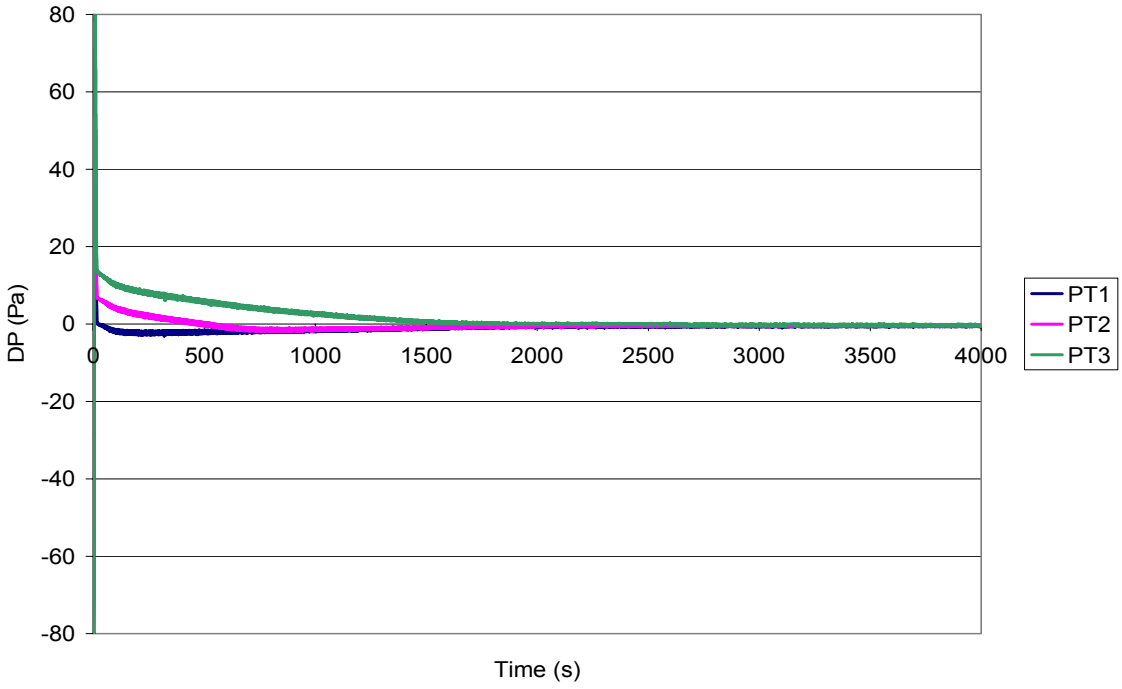

Figure A 21: Experiment 080305_Test2 Pressure Profiles A_o=0.000127 m^2 A_i=0.00038 m^2

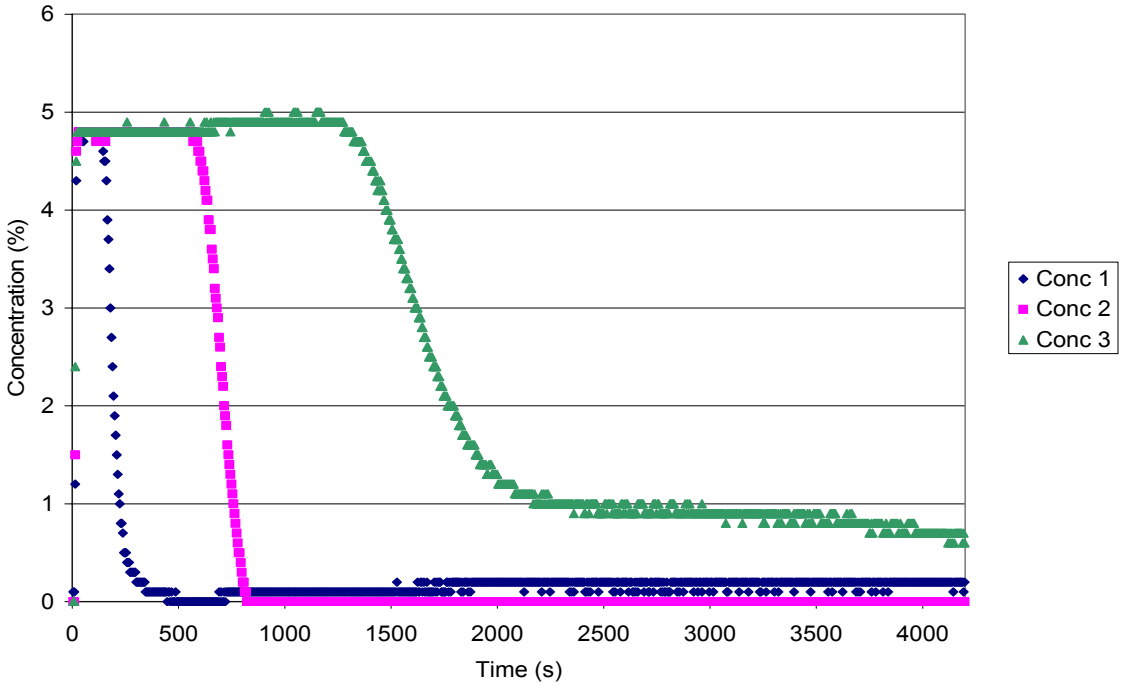

Figure A 22 Experiment 080305_Test2 Concentration Profiles A_o=0.000127 m^2 A_i=0.00038 m^2

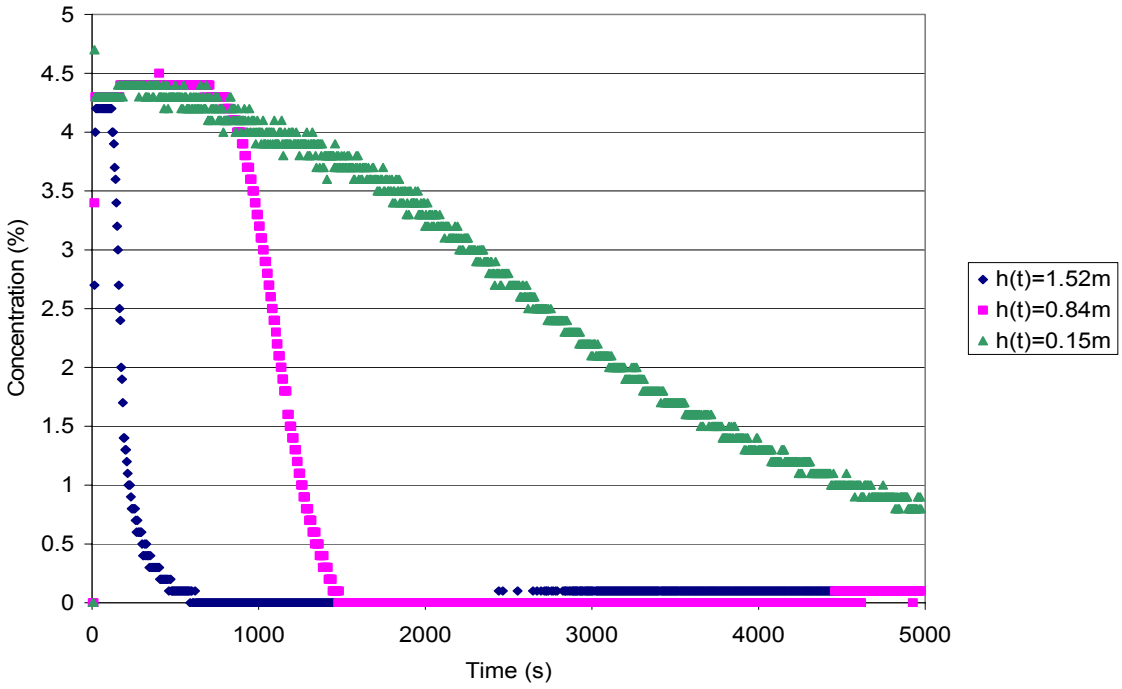

Figure A 23 Experiment 080405_Test4 Concentration Profiles A_o=0.00038 m^2 A_i=0.000127 m^2

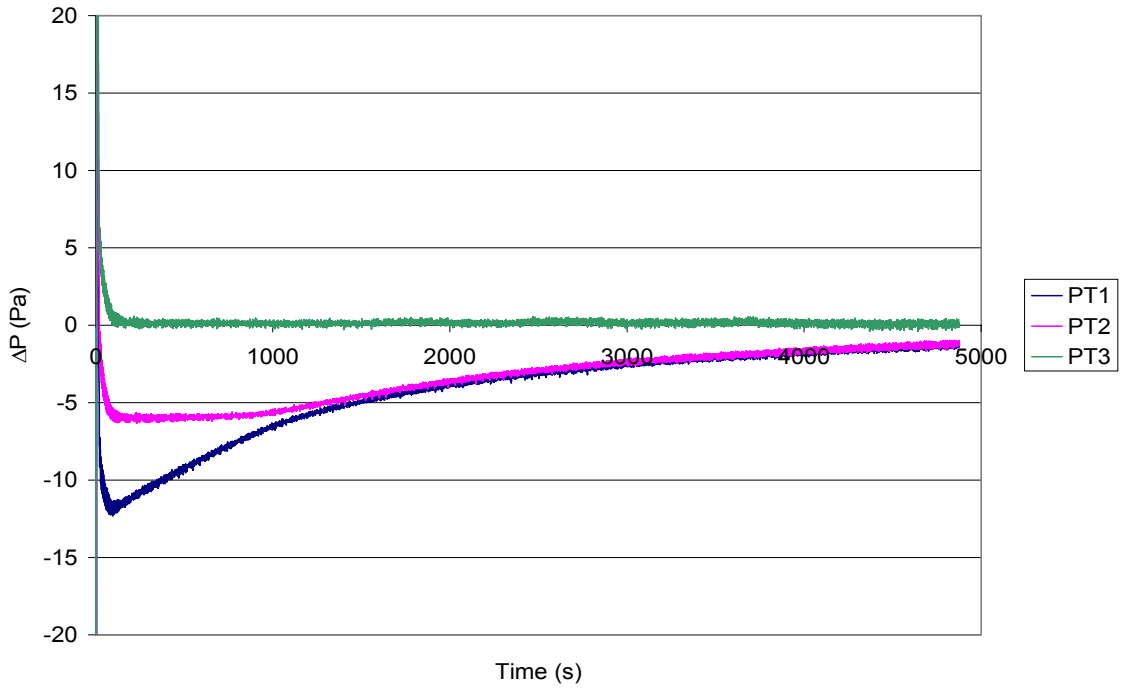

Figure A 24 Experiment 080405_Test5 Pressure Profiles A_o=0.00038 m^2 A_i=0.000127 m^2

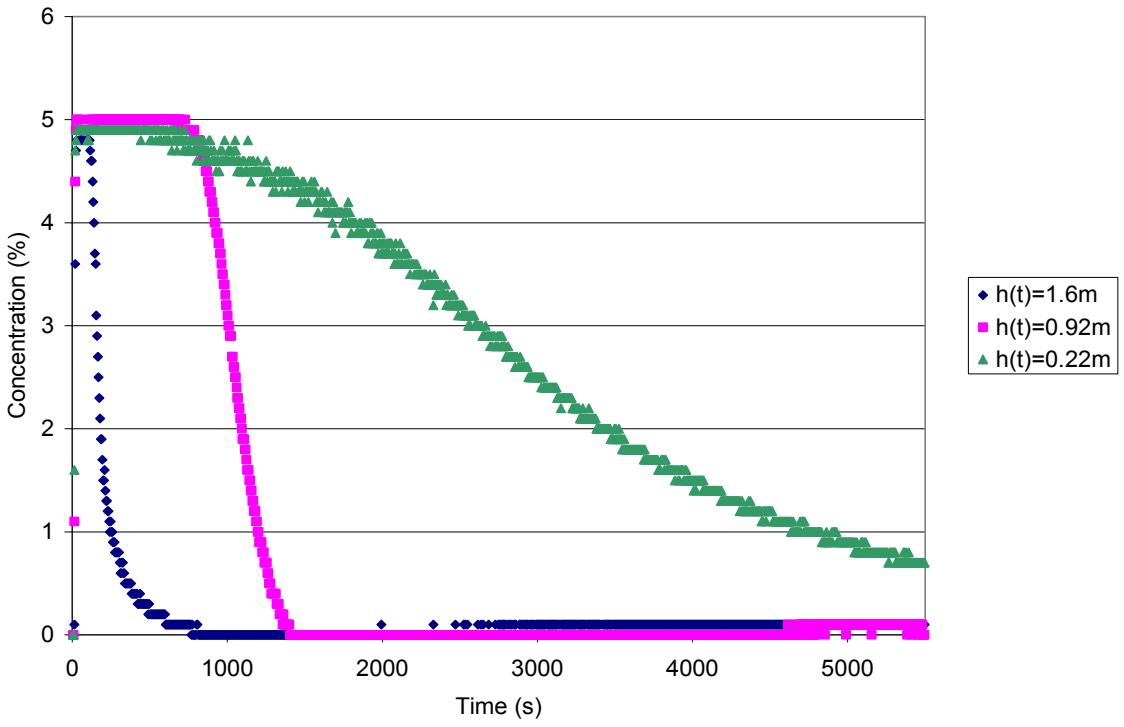

Figure A 25 Experiment 080405_Test5 Concentration Profiles A_o=0.000127 m^2 A_i=0.00038 m^2

Appendix B: Pressure Transducer Calibration Curves

Three pressure transducers were placed at h(t) heights of 1.68, 0.84, and 0 m to measure the hydrostatic pressure differences between the inside and outside of the enclosure. After the initial pressure surges, these pressure differences ranged from 0-20 PA. Due to the small pressure variations it is important that the pressure transducers are correctly calibrated. The calibration curves for the pressure transducers are shown below.

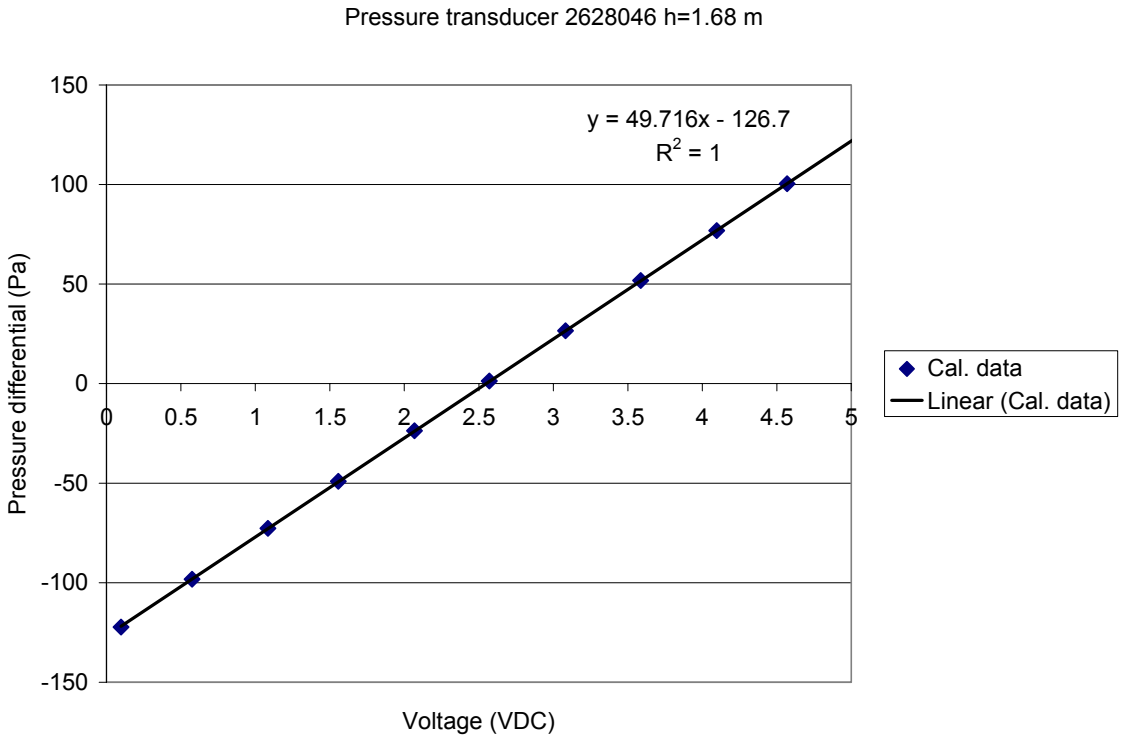

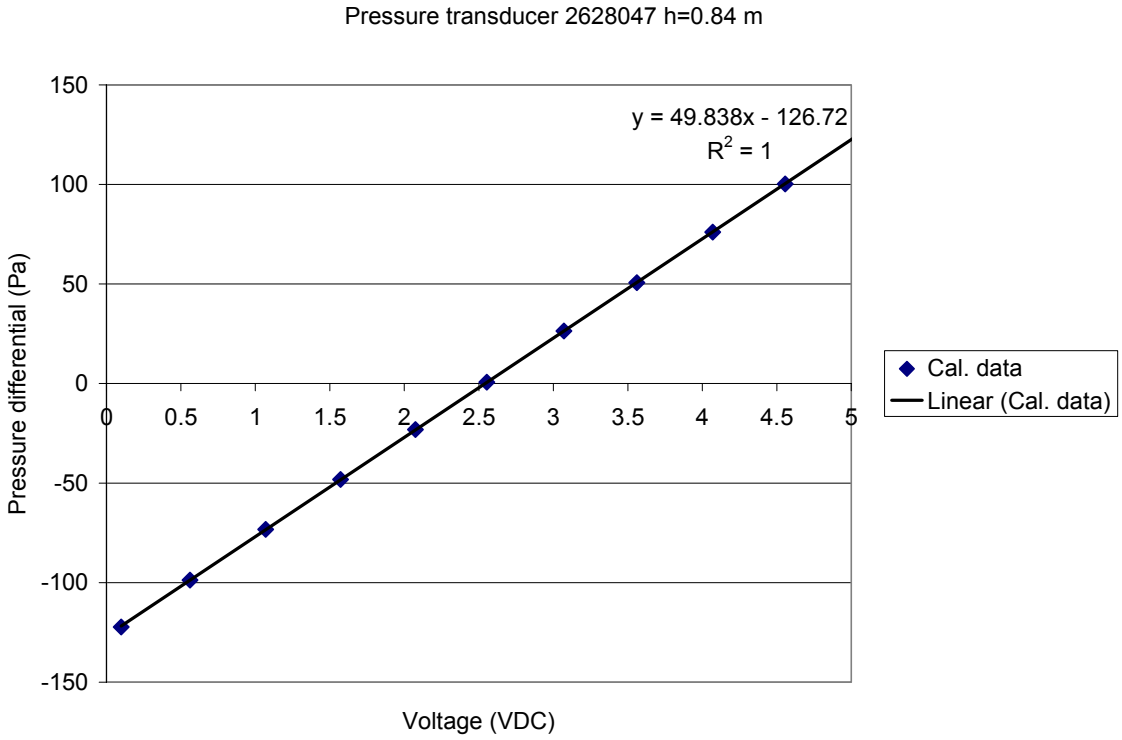
Pressure transducer 2628047 h=0.84 m
y = 49.838x - 126.72
R2 = 1
150
100
50
0
-50
-100
-150
0
0.5
1
1.5
2
2.5
3
3.5
4
4.5
5
Pressure differential (Pa)
Voltage (VDC)
Cal. data
Linear (Cal. data)

References

3M, "Novec 1230 Brochure", 3M Specialty Materials Division, 2003 http://www.3m.com/novec1230fluid

Dewsbury J., and Whiteley, R. A., "Extensions to standard hold time calculations," *Fire Technology*, Vol. 36, No. 4, 2000, pp 266- 278.

Dewsbury J., and Whiteley, R. A., "Review of fan integrity testing and hold time standards," *Fire Technology*, Vol. 36, No. 4, 2000, pp 249- 265.

Dewsbury J., and Whiteley, R. A., "Hold time calculations for non-standard enclosures," *Fire Technology*, Vol. 40, 2004, pp 78-89.

DiNenno, P., Halon Replacement Clean Agent Total Flooding Systems The SFPE Handbook of Fire Protection Engineering 3rd Ed, Society of Fire Protection Engineers, 2002 pp 4-173-4-198.

DiNenno, P. J., and Forssell, E. W. "Evaluation of the door fan pressurization leakage test method applied to Halon 1301 total flooding systems," *Journal of Fire Protection Engineering*, Vol. 1, No. 4, 1989, pp 131-140.

ISO/fDIS 1450.1 Gaseous fire extinguishing systems – Physical properties and system design, Part 1: General Requirements, Annex E, International Standards Organization, 2003.

Klocke, M., Door-fan-test Proceedings of Congress on Fire Extinguishing Systems, VdS, Cologne, Germany, December 1998.

Myint L.S., *Methodologies for limiting emissions of halogenated fire extinguishant agents for enclosures*, Ph.D. thesis, University of Manchester Faculty of Technology (UMIST), Manchester, England ,1991.

NFPA 2001, Standard on clean agent fire extinguishing systems, National Fire Protection Association, 2004